Circ_0030998 Promotes Tumor Proliferation and Angiogenesis by Sponging miR-567 to Regulate VEGFA in Colorectal Cancer

Longyang Jin
Department of Colorectal Surgery, the Sixth Affiliated Hospital of Sun Yet-Sen University, Guangzhou, Guangdong.

Chao Han
Department of General Surgery, Shanghai General Hospital, Shanghai Jiaotong University school of Medicine, Shanghai, China.

Tianyu Zhai
Department of General Surgery, Xinhua Hospital, Shanghai Jiaotong University School of Medicine, Shanghai, China.

Xiaoyu Zhang
Department of General Surgery, Xinhua Hospital, Shanghai Jiaotong University School of Medicine, Shanghai, China.

Chun Chen
Department of Colorectal Surgery, the Sixth Affiliated Hospital of Sun Yet-Sen University, Guangzhou, Guangdong.

Lei Lian (✉ lianlei2@mail.sysu.edu.cn)
Department of Colorectal Surgery, the Sixth Affiliated Hospital of Sun Yet-Sen University, Guangzhou, Guangdong.

Research

Keywords: Circ_0030998, Colorectal cancer, miR-567, VEGFA, proliferation

Posted Date: October 20th, 2020

DOI: https://doi.org/10.21203/rs.3.rs-92165/v1

Abstract

Background

Colorectal cancer (CRC) is one of the most common malignancies worldwide. Accumulating studies have demonstrated that circular RNAs (circRNAs), a novel class of noncoding RNAs, are involved in pathological processes, especially in the development of cancers. But the roles of circRNAs in CRC are largely unknown.

Methods

The microarray data GSE138589 was analyzed and qRT-PCR was performed to screen out the circRNA with the highest upregulated level in CRC. QRT-PCR was used to determine the expression of genes in different tissues or cells. RNA-FISH was conducted to identify the subcellular localization of Circ_0030998. In vitro and in vivo assays were performed to determine the effect of Circ_0030998 on the CRC cells proliferation and angiogenesis. The relationships of Circ_0030998, miR-567 and VEGFA were predicted and validated using bioinformatic tools, RIP and luciferase assays.

Results

We identified a novel circRNA, Circ_0030998, was upregulated in CRC tissues and cells, and its upregulation was related with poor prognosis in CRC patients. Circ_0030998 promoted CRC cells proliferation and angiogenesis. RNA-FISH showed that Circ_0030998 was mainly localized in the cytoplasm of CRC cells. Mechanistic studies demonstrated that Circ_0030998 acted as a miR-567 sponge to relieve its inhibitory effect on VEGFA. Rescue assays validated that Circ_0030998 functioned in CRC cells proliferation and angiogenesis relying on VEGFA.

Conclusions

The present study clarified the Circ_0030998/miR-567/VEGFA regulation axis and indicated that Circ_0030998 could be a potential therapeutic target for CRC.

Background

Colorectal cancer (CRC), one of the most common malignancies, has become the third leading cause of cancer-related deaths worldwide[1]. Even with the popularity of colonoscopy and practice of advanced treatments including chemotherapy, radiotherapy and immunotherapy, the overall survival of CRC patients has not increased significantly[2]. For patients of stage IV, the prognosis is extremely poor with a 5-year survival rate of less than 20%[3]. Although more and more oncogenes have been identified in the occurrence and development of CRC, the specific mechanisms are still obscure. So it's urgently needed to explore the molecular mechanisms related with the progression of CRC.

Only about 1.5% of the human genome contains protein-coding genes, with the majority of the remaining transcribed into non-coding RNAs[4]. Accumulating studies have demonstrated that non-coding RNAs play important roles in the body's growth, disease, aging, reproduction and other physiological and pathological processes[5]. In terms of species complexity, non-coding genes may function more importantly than protein-coding genes[6]. Circular RNAs (circRNAs), characterized with a covalently closed loop, were first found in RNA virus in 1970s[7], and were initially regarded as by-products of splicing from exons or introns of host genes[8]. However, more and more studies have shown that circRNAs are involved in pathological processes and could regulate gene expression in various ways[9]. CircRNAs could function as competing endogenous RNAs by sponging microRNAs to regulate genes expression. For example, circ_0020710 could promote melanoma cell proliferation, migration and invasion by sponging miR-370-3p and then regulating the CXCL12 expression[10]. CircRNAs could also bind with RNA binding proteins (RBPs) directly, and affect the function of RBPs[11]. Some circRNAs could regulate the expression of host genes by interacting with RNA polymerase II[12]. A small part of circRNAs could even act as protein templates[13, 14, 15]. The covalently closed loop structure of circRNAs resulted in the high stability, which helped them to be ideal biomarkers. Several circRNAs have been detected involved in the progression of colorectal cancer[16, 17, 18]. However, identification of more functional circRNAs may facilitate the molecular-guided diagnosis and treatment of colorectal cancer.

In the present study, We identified a new circular RNA, Circ_0030998, which has never been reported in the literature, functioned as an oncogene in the proliferation and angiogenesis of CRC. Circ_0030998 was derived from the exon 3 of host gene LAMP1 and upregulated in CRC tissues and cell lines compared with nontumor tissues and non-tumorigenic colorectal epithelial cell line. High expression of Circ_0030998 was related with lymph node metastasis, TNM stage and poor prognosis of CRC patients. Moreover, Circ_0030998 could promote CRC cells proliferation *in vitro* and *in vivo*. Mechanistically, Circ_0030998 acted as a miR-567 sponge to relieve the inhibitory effect of miR-567 on VEGFA, which played important roles in the proliferation and angiogenesis of CRC. In summary, the present study explored the mechanism of Circ_0030998 in the progression of CRC, demonstrated the Circ_0030998/miR-567/VEGFA axis and provided a new potential target for the treatment against CRC.

Materials And Methods

Collection of clinical data and tissue specimens

A total of 90 paired CRC tissues and neighbouring nontumor tissues were obtained from patients diagnosed as CRC after surgery in Shanghai General Hospital (Shanghai Jiaotong University School of Medicine, Shanghai, China) from 2010 to 2014. None of the patients received any chemotherapy or radiotherapy before the surgery. Complete clinicopathological data was collected from every patient. All tissues were stored in liquid nitrogen before RNA extraction. The study was approved by the Human Ethics Committee of Shanghai General Hospital, and every patient signed the informed consent.

Cell culture

All the human CRC cell lines (HT29, SW620, DLD-1, HCT116, SW480, LoVo) and a human non-tumorigenic colorectal epithelial cell line (NCM460) were purchased from the Cell Bank of the Chinese Academy of Science (Shanghai, China). McCoy's 5A complete medium (Gibco, USA) was used for the culture of HT29, HCT116; RPMI-1640 medium (Gibco, USA) was used for the culture of SW620, DLD-1, LoVo, NCM460, SW480. All the cells were cultured in the medium containing 10% fetal bovine serum (Gibco, USA) at 37°C with 5% CO_2.

QRT-PCR assay

RNA was extracted from tissues or cells with TRIzol reagent (Invitrogen, USA), then Primer-Script One Step RT-PCR kit (TaKaRa, China) was used for reverse transcription and SYBR Premix Dimmer Eraser kit (TaKaRa, China) was used for RT-PCR. All the primers used in the present study were designed by Shanghai Sangon Biotech Co.Ltd and shown in Supplementary Table 1. GAPDH was used for normalization and the relative expression fold changes of RNAs was calculated with the $2^{-\Delta\Delta Ct}$ method. All the assays were performed in triplicate.

RNA fluorescence in situ hybridization (RNA-FISH)

Cy3-labeled probe for Circ_0030998 was designed and generated by RiboBio (Guangzhou, China) and Fluorescent in Situ Hybridization kit (RiboBio, China) was used for the identification of the subcellular localization of Circ_0030998 according to the manufacturer's recommendations. After co-staining with DAPI for the cell nuclei, the images were acquired.

Cell transfection

The sequences of small interference RNAs for Circ_0030998, VEGFA and scrambled negative control (NC) siRNAs were designed and synthesized by GenePharma (Shanghai, China). MiR-567mimics, miR-567 inhibitors and miR-NC were purchased from Shanghai Sangon Biotech Co.Ltd. Circ_0030998 and VEGFA cDNA were amplified and cloned into pcDNA3.0 vector (Invitrogen) for ectopic overexpression. The small hairpin RNA (shRNA) of Circ_0030998 was designed and synthesized from GenePharma (Shanghai, China). QRT-PCR was conducted to examine the amplification and knockdown efficiencies. The sequences of siRNAs and shRNA used in the present study was shown in Supplementary Table 1.

Cell counting kit-8 (CCK-8) assay

The ability of CRC cells proliferation was examined using CCK-8 kit (Beyotime, China). 1×10^3 transfected CRC cells were seeded into each well of 96-well plate, and the absorbance at 450nm was measured every 24h for 96h. Each group was cultured in five replicate wells and all assays were conducted in triplicate.

Colony formation assay

200 transfected CRC cells were seeded into each well of six-well plate. After incubation for two weeks, the cells were fixed with 4% paraformaldehyde and stained with 0.1% crystal violet. Then the numbers of the colonies were counted by visual inspection and all the assays were conducted in triplicate.

Flow cytometric analysis

All the transfected CRC cells were harvested after incubation for 48h. Then the cells were fixed in pre-chilled 70% ethanol for 16h at 4℃ and Cell Cycle Analysis Kit (Beyotime, China) was used to stain cells for 30 minutes with propidium iodide according to the protocol. Flow cytometry (BD Biosciences, USA) was used for cell cycle analysis at last and all the assays were performed in triplicate.

Tube formation assay

Red fluorescent proteins (RFP) expressing human umbilical vein endothelial cells (HUVECs) were obtained from Angio-Proteomie (Boston, USA) and cultured in endothelial growth medium (EGM-2) and passage 5 was used for the experiments. 50μl of precooled Matrigel (BD, Corning, USA) was coated into each well of a 96-well plate and polymerized for 30min at 37°C. Next, 2×10^4 HUVEC-RFP cells were suspended in a mixture of conditioned medium (50μl) and endothelial cell medium (50μl) containing 10% FBS. The fluorescence detection of tube formation was photographed using a inverted microscopy (IX-53, Olympus) after 6h of incubation at 37°C.

Bioinformatics analysis

Two bioinformatics databases, circBank (http://www.circbank.cn/index.html) and Circular RNA Interactome (https://circinteractome.nia.nih.gov/), were used to screen for miRNAs that could bind with Circ_0030998. Three miRNA databases, miRTarBase (http://mirtarbase.mbc.nctu.edu.tw/php/index.php), DIANA TOOLS (http://diana.imis.athena-innovation.gr/DianaTools/index.php) and miRDB (http://www.mirdb.org/) were used to predict the potential target genes of miR-567 in the present study.

Luciferase reporter assay

The putative binding sequences and mutant sequences of miR-567 in Circ_0030998 and VEGFA 3'-UTR were amplified and inserted into pGL3-promoter vector to generate luciferase reporter constructs (GenePharma, China). Then the CRC cells were co-transfected with luciferase reporter constructs and miR-567mimics or miR-NC. After incubation for 48h, the renilla and firefly luciferase activities were measured by the Dual-Luciferase Reporter Assay System (Promega).

RNA immunoprecipitation (RIP)

HCT116 and SW480 cells transfected with miR-567 mimic or miR-NC were lysed in RIP lysis buffer. The Magna RNA immunoprecipitation kit (Millipore, USA) was used to examine the combination of Circ_0030998 and miR-567 according to the manufacturer's protocol. The magnetic beads pre-coated

with antibody against Ago2 or IgG were used for precipitation. QRT-PCR was performed to quantify the level of Circ_0030998 enriched by RIP.

Western blotting

RIPA lysis buffer and protease inhibitor cocktail were used for the extraction of total proteins from cells. BCA Protein Assay Kit (Beyotime, China) was used to determine the protein concentrations. Then the protein lysates were separated by SDS-PAGE and transferred to PVDF membranes. After incubation with primary antibodies at 4°C overnight, the membranes were incubated with the corresponding secondary antibodies at room temperature for 1h. Finally, the proteins were evaluated by chemiluminescence according to the manufacturer's instructions. Antibodies used in the present study were: VEGFA (26381-1-AP, Proteintech), β-actin (60008-1-Ig, Proteintech). All assays were performed in triplicate.

Animal experiment

Four-week-old male athymic BALB/c nude mice were used in the present study. Ten mice were randomly divided into two groups and injected subcutaneously with SW480 cells (100μl, 1×10^6) transfected with either sh-NC or sh-Circ_0030998 in the left flank. Then, all the mice were maintained under specific-pathogen-free conditions and the tumor volumes were measured as $0.5\times length\times width^2$ weekly. Four weeks later, all the mice were sacrificed and all the tumors were excised. The study was approved by the Animal Care and Use Committee of Shanghai General Hospital.

Statistical analysis

All the continuous data was shown as mean ± standard deviation. Student's t-test or One-way ANOVA was applied to compare group differences. χ^2 test was used to evaluate the correlation between clinicopathologic characters and Circ_0030998 expression. For survival analysis, Kaplan-Meier method with the log-rank test was conducted. Univariate and multivariate Cox proportional hazards models were performed to analyze the prognostic factors. All the statistical analyses were completed using SPSS 20.0 and a two-sided *p* value less than 0.05 was considered statistically significant.

Results

Identification of Circ_0030998

By analyzing the microarray data GSE138589, which compared six pairs of CRC tissues and matched neighboring normal tissues. A total of 155 upregulated circRNAs and 29 downregulated circRNAs with *p* value < 0.05 and |fold change| > 1 were identified (Supplementary Table 2). The differently expressed circRNAs were exhibited by volcano plots as shown in Figure 1A. Among these 184 circRNAs, the top 30 ones (21 upregulated and 9 downregulated) with the most significant differences were selected for further study and shown by hierarchical clustering analysis in Figure 1B. To screen out the circRNA that may be related to the progression of CRC cells, the expression of 21 upregulated circRNAs were tested in

CRC tissues, and it was shown that Circ_0030998 had the highest level than other 20 circRNAs (data not shown). Therefore, we chose Circ_0030998 for further analysis.

According to the circBase (http://www.circbase.org/) and UCSC Genome Browser Home (http://genome.ucsc.edu/), we found that Circ_0030998 was 220 base pairs (bp) in length located at chr13:113963957-113964177 and it was derived from the exon 3 of host gene LAMP1, which acted as an oncogene in the progression of several cancers[19, 20].

Circ_0030998 was significantly upregulated in CRC tissues and associated with poor prognosis of CRC patients

Firstly, qRT-PCR was performed to identify the expression levels of Circ_0030998 in 90 pairs of CRC tissues and adjacent normal tissues. As shown in Figure 1C, Circ_0030998 was significantly upregulated in CRC tissues compared to the adjacent normal tissues. Moreover, we divided 90 CRC patients into two groups according to the median level (cutoff value = 2.961) of the relative Circ_0030998 expression in tumor tissues: the high group (n = 45) and the low group (n = 45). Then Pearson chi-square tests were used to analyze the relationship between Circ_0030998 expression level and patients' clinicopathologic features. It was demonstrated that high expression of Circ_0030998 was related with lymph node metastasis and TNM stage but not gender, age, tumor location, CEA level and tumor size of CRC patients (Table 1).

Furthermore, Kaplan-Meier survival analysis was conducted to analyze the relationship between Circ_0030998 expression level and patients' survival. It showed that patients with high Circ_0030998 levels had a shorter survival compared to those with low levels (Figure 1D). Univariate survival analysis showed that lymph node metastasis, TNM stage and Circ_0030998 expression were prognostic factors. Multivariate Cox regression analysis demonstrated that only TNM stage and Circ_0030998 expression were independent prognostic factors for CRC patients (Table 2).

Circ_0030998 was upregulated in CRC cell lines and promoted tumor proliferation and angiogenesis *in vitro*

The relationship of Circ_0030998 expression and prognosis of CRC patients suggested that Circ_0030998 was correlated with tumor malignancy. Thus, we investigated the functions of Circ_0030998 in CRC cell lines. Fist, we examined the expression of Circ_0030998 in six CRC cell lines (HT29, SW620, DLD-1, HCT116, SW480, LoVo) and a human non-tumorigenic colorectal epithelial cell line (NCM460) by qRT-PCR. The results showed that Circ_0030998 was significantly upregulated in CRC cell lines than NCM460 (Figure 2A). Then, the SW480 cell line which had the relatively highest expression of Circ_0030998 and HCT116 cell line which had the relatively lowest expression of Circ_0030998 were chosen for further study. Two siRNAs targeting Circ_0030998 were transfected into SW480, and si-Circ_0030998-1 which was chosen for subsequent experiments exhibited better knockdown efficiency (Figure 2B). Meanwhile, Circ_0030998 overexpression plasmid significantly upregulated the expression of Circ_0030998 in HCT116 cells (Figure 2C).

Then, RNA fluorescence in situ hybridization assays with specific Cy3-labeled probe for Circ_0030998 were performed to identify the subcellular localization of Circ_0030998, and the results demonstrated that Circ_0030998 was mainly localized in the cytoplasm of SW480 and HCT116 cells (Figure 2D). Next, CCK-8 and colony formation assays showed that downregulation of Circ_0030998 significantly inhibited the proliferation and the cloning ability of SW480 cells; whereas, overexpression of Circ_0030998 promoted these functions in HCT116 cells (Figure 3A and 3B). Moreover, flow cytometry analyses showed that Circ_0030998 downregulation led to a significant G1/G0 phase arrest in SW480 cells and vice versa in HCT116 cells when Circ_0030998 was overexpressed (Figure 3C). Furthermore, HUVECs were used to examine the effect of Circ_0030998 on angiogenesis, and the results showed that the formation of tube-like structures were significantly inhibited when Circ_0030998 was downregulated and vice versa when Circ_0030998 was overexpressed (Figure 3D). These results suggested that Circ_0030998 acted as an oncogene that promoted the CRC cells proliferation and angiogenesis.

Downregulation of Circ_0030998 inhibited CRC growth *in vivo*

To further confirm the roles of Circ_0030998 on tumorigenesis *in vivo*, shRNA targeting Circ_0030998 was constructed, and the significant knockdown efficiency of sh-Circ_0030998 was verified by qRT-PCR as shown in Figure 4A. Then, SW480 cells transfected with either sh-NC or sh-Circ_0030998 were injected subcutaneously in the left flank of nude mice. As shown in Figure 4B and 4C, the tumor volumes in the sh-Circ_0030998 group were obviously smaller than those in the sh-NC group. Meanwhile, the Circ_0030998 expression in tissues from sh-Circ_0030998 group was significantly lower than that from sh-NC group (Figure 4D). These data suggested that knockdown of Circ_0030998 could inhibit CRC cells proliferation *in vivo*.

Circ_0030998 facilitated CRC cells proliferation and angiogenesis by spongingmiR-567

Many studies have revealed that circRNAs functioned as “miRNA sponges”, namely, competing endogenous RNAs (ceRNAs), to block the formation of Ago2-mediated silencing complex. Because Circ_0030998 was mainly localized in the cytoplasm of CRC cells, we supposed that Circ_0030998 may also function as a ceRNA. Then two bioinformatics databases, circBank (http://www.circbank.cn/index.html) and Circular RNA Interactome (https://circinteractome.nia.nih.gov/), were used to screen for miRNAs that could bind with Circ_0030998. As shown in the Supplementary Table 3, only miR-567 and miR-556-5p were both predicted by two databases. QRT-PCR showed that only miR-567 was upregulated in SW480 cells when Circ_0030998 was knockdown (data not shown); furthermore, we examined miR-567 expression in 90 CRC tissues, and a significant inverse correlation was found between miR-567 and Circ_0030998 as shown in Figure 5A; so we hypothesized that miR-567 was the miRNA sponged by Circ_0030998.

To further validate whether Circ_0030998 could interact with miR-567 directly in CRC cells, the wildtype and mutated putative binding sites of Circ_0030998 were cloned and inserted into luciferase reporter vectors respectively for luciferase reporter assays (Figure 5B). The results showed that the luciferase activity of the wildtype but not mutant Circ_0030998 was significantly inhibited by miR-567 mimics in

both SW480 and HCT116 cells (Figure 5C). Furthermore, the RIP assays demonstrated that miR-567 significantly increased the enrichment of Circ_0030998 by Ago2 RIP in both SW480 and HCT116 cells compared to miR-NC (Figure 5D). These results suggested that Circ_0030998 functioned as a ceRNA for miR-567 in CRC cells.

Next, we examined the effect of miR-567 on CRC cells proliferation and angiogenesis. CCK-8 and colony formation assays showed that downregulation of miR-567 by miR-567 inhibitor increased HCT116 cells proliferation (Figure 5E and 5F). Flow cytometry analyses demonstrated that miR-567 inhibitor promoted HCT116 cells cycle progression (Figure 5G). Moreover, inhibition of miR-567 increased the tube-like structures formation of HUVECs (Figure 5H).

Furthermore, we performed rescue assays to confirm whether Circ_0030998 regulated CRC cells proliferation and angiogenesis via miR-567. CCK-8 and colony formation assays showed that miR-567 mimic could partially weaken the promotive effect of Circ_0030998 on HCT116 cells proliferation (Figure 6A and 6B). MiR-567 mimic also reversed the promotive effect of Circ_0030998 on HCT116 cells cycle progression and tube-like structures formation of HUVECs (Figure 6C and 6D). Taken together, these results suggested that Circ_0030998 promoted CRC cells proliferation and angiogenesis via miR-567.

MiR-567 inhibited CRC cells proliferation and angiogenesis via VEGFA

MiRNAs could regulate target mRNAs by binding with their 3'UTRs via complementary base pairing. Previous studies showed that miR-567 could regulate KPNA4[21], ATG5[22] and then inhibited tumor progression or chemoresistance. To explore the mechanism by which miR-567 inhibited CRC cells proliferation and angiogenesis, three miRNA databases were used to predict the potential target genes in the present study. As shown in Figure 7A and Supplementary Table 4, there were 10 potential target genes in the overlapped fraction of three databases, namely BNC2, BVES, CSRNP3, KANSL1L, MB21D2, MBNL2, NEUROD2, UBR3, VEGFA, ZSWIM6. Among these 10 candidate genes, only VEGFA could promote cancer proliferation and angiogenesis. So we hypothesized that VEGFA may be the downstream target gene of miR-567 in regulating CRC cells proliferation and angiogenesis.

Then, we examined miR-567 and VEGFA expression in 90 CRC tissues, and it showed that VEGFA expression was negatively correlated with miR-567 in CRC tissues (Figure 7B). To further confirm the interaction between miR-567 and VEGFA, we performed luciferase reporter assays with luciferase reporter vectors containing the wildtype or mutated putative binding sites of VEGFA (Figure 7C). The results showed that the luciferase activity of the wildtype VEGFA was significantly inhibited by miR-567 mimics in both SW480 and HCT116 cells compared with mutant VEGFA (Figure 7D).

Moreover, we designed pcDNA-VEGFA for ectopic expression to verify the effect of VEGFA on CRC cells proliferation and angiogenesis. The efficiency of pcDNA-VEGFA was examined by qRT-PCR as shown in Figure 7E. CCK-8 and colony formation assays showed that overexpression of VEGFA promoted HCT116 cells proliferation (Figure 7F and 7G). Flow cytometry analyses demonstrated that VEGFA promoted HCT116 cells cycle progression (Figure 7H). Meanwhile, VEGFA promoted the tube-like structures

formation of HUVECs (Figure 7I). The effect of VEGFA on HCT116 cells and HUVECs coincided with that of miR-567 inhibitor. These findings suggested that miR-567 inhibited CRC cells proliferation and angiogenesis via VEGFA.

Circ_0030998 promoted CRC cell proliferation and angiogenesis via themiR-567/VEGFA axis

Furthermore, western blotting showed that VEGFA was decreased in SW480 transfected with si-Circ_0030998, and vice versa in HCT116 cells when Circ_0030998 was overexpressed (Figure 8A). We also designed si-VEGFA and conducted rescue assays to confirm whether Circ_0030998 functioned in CRC via VEGFA. CCK-8 and colony formation assays showed that the effect of Circ_0030998 on HCT116 cells proliferation was partially reversed by si-VEGFA (Figure 8B and 8 C). Si-VEGFA also weakened the promotive effect of Circ_0030998 on HCT116 cells cycle progression and tube-like structures formation of HUVECs (Figure 8D and 8 E). All these data suggested that Circ_0030998 promoted CRC cells proliferation and angiogenesis via the miR-567/VEGFA axis.

Discussion

Till now, more than 100,000 human circRNAs have been discovered[23, 24], and many of them have been detected playing important roles in various physiological and pathological processes such as cell differentiation[25], cell cycle progression[26], cellular proliferation[27], apoptosis of cancer cells[28], immune tolerance[29] and so on. Several circRNAs have been validated effective in the progression of CRC[16, 17, 18]. In the present study, we analyzed the microarray data GSE138589, which compared differentially expressed circRNAs in six pairs of CRC tissues and matched neighboring normal tissues, and confirmed a new circRNA, Circ_0030998, was upregulated in CRC tissues. The dysregulation of Circ_0030998 was related with CRC patients' survival, suggesting its potential diagnostic and therapeutic value as a biomarker. Moreover, Circ_0030998 significantly regulated CRC cells proliferation *in vitro* and *in vivo*, and also affected the tube formation of HUVECs.

CircRNAs are formed by back-splicing of primary transcripts in nucleus and then transported to the cytoplasm via ATP-dependent RNA helicase DDX39A and spliceosome RNA helicase DDX39B[30]. RNA fluorescence in situ hybridization was an effective method for the visualization of circRNA. In the present study, we identified that Circ_0030998 was mainly localized in the cytoplasm of CRC cells by FISH, which indicated that Circ_0030998 may function as a miRNA sponge. Accumulating studies have demonstrated that circRNAs in cytoplasm mainly played their roles as competing endogenous RNAs[31, 32]. MiR-567 was predicted by bioinformatics analysis and further validated by luciferase reporter assay as the target miRNA of Circ_0030998 in our study. Furthermore, a negative correlation between miR-567 and Circ_0030998 was detected in CRC tissues. All these data suggested that Circ_0030998 served as a ceRNA in the regulation of CRC proliferation and angiogenesis.

MicroRNAs (miRNAs), approximately 21-23nt in length, mainly play a post-transcriptional regulatory role in gene expression. The mature miRNAs in cytoplasm bind with Argonaute protein family members and

then the miRNA-induced silencing complex (miRISC) forms[33]. This complex binds to the 3' untranslated region of the target mRNA through miRNA according to the principle of base pairing, thereby exerting an inhibitory or silencing effect[34, 35]. MiR-567, a tumor suppressor gene, has been studied in several cancers. In breast cancer, miR-567 could inhibit cancer cells proliferation and migration by regulating KPNA4[21]; miR-567 could also regulate autophagy and reverse trastuzumab resistance via ATG5 in breast cancer[22]; in renal cell carcinoma, miR-567 could inhibit cancer cells progression by regulating PRDX3[36]. Consistent with the reported studies, we found that inhibition of miR-567 could promote CRC cells proliferation and angiogenesis. Moreover, overexpression of miR-567 could partially reverse the effect of Circ_0030998 on CRC cells and HUVECs. Next, we predicted the target mRNA of miR-567 by three bioinformatic algorithms (miRTarBase, miRDB and DIANA TOOLS), and confirmed that VEGFA was a target of miR-567 by luciferase reporter assay.

Angiogenesis is an important factor in the solid tumor progression, and anti-angiogenesis has been demonstrated effective in cancer therapy[37]. VEGFA is a primary factor driving the tumour vascular formation[38, 39]. In tumor tissues, a variety of cells can produce VEGFA, such as cancer cells, endothelial cells and tumour-associated macrophages[40]. VEGFA mainly functions by binding to the receptors, especially VEGFR2, and activates the VEGFR2-dependent signaling pathways[41]. Moreover, VEGFA can accelerate tumor progression by promoting EMT and metastasis[42]. In patients with colorectal cancer liver metastasis, VEGFA could be a prognostic biomarker[43]. In the present study, VEGFA was predicted and validated to be the target of miR-567. Overexpression of VEGFA promoted CRC cells proliferation and cell cycle progression, induced the tube-like structures formation of HUVECs. Furthermore, VEGFA was found to be in positive correlation with Circ_0030998 in CRC cells. Rescue assays demonstrated that the effects of Circ_0030998 on CRC cells proliferation and tube formation of HUVECs could be partially reversed by VEGFA downregulation. Altogether, our data suggested that Circ_0030998 functioned in CRC proliferation and angiogenesis by regulating VEGFA via miR-567.

Conclusions

In conclusion, the present study identified the high expression of Circ_0030998 in CRC tissues and cell lines, revealed the relationship between Circ_0030998 and clinicopathologic features, prognosis of CRC patients. Moreover, Circ_0030998 served as a ceRNA for miR-567 and then relieved the inhibitory effect of miR-567 on VEGFA, resulting in the proliferation and angiogenesis of CRC eventually. Our findings demonstrated the Circ_0030998/miR-567/VEGFA regulation axis in CRC and suggested that Circ_0030998 could be a potential therapeutic target for CRC.

Abbreviations

CRC: Colorectal cancer; CXCL12: CXC chemokine ligand 12; LAMP1: lysosomal-associated membrane protein 1; TNM: Tumor Node Metastasis; VEGFA: vascular endothelial growth factor A; HUVEC: human umbilical vein endothelial cell; ceRNA: competing endogenous RNA; UTR: Untranslated Region; KPNA4:

karyopherin subunit alpha 4; ATG5: autophagy-related 5; BNC2: basonuclin 2; BVES: blood vessel epicardial substance; CSRNP3: cysteine and serine rich nuclear protein 3; KANSL1L: KAT8 regulatory NSL complex subunit 1-like protein; MB21D2: *Mab-21 domain-containing protein 2;* MBNL2: muscleblind-like protein 2; NEUROD2: neuronal differentiation-2; UBR3: ubiquitin-binding region 3; ZSWIM6: Zinc finger SWIM domain containing protein 6; PRDX3: peroxiredoxin 3; EMT: Epithelial-to-mesenchymal transition.

Declarations

Ethics approval and consent to participate

The present study was approved by the Human Ethics Committee of Shanghai General Hospital (Shanghai Jiaotong University School of Medicine, Shanghai, China). Informed consent was obtained from all patients involved in the study. The animal experiments were approved by the Animal Care and Use Committee of Shanghai General Hospital.

Consent for publication

All authors agree the publication of the present study.

Availability of data and materials

All data presented in the study is available from the corresponding author on reasonable request.

Competing interests

All authors declare that there are no competing financial interests.

Funding

None.

Authors' contributions

LY J, C H conducted the majority of the molecular and cellular experiments, drafted the manuscript. TY Z and XY Z collected the clinical data and performed the animal experiments. C C, L L organized the study, carried out the statistical analyses and modified the manuscript. All authors read and approved the final manuscript.

Acknowledgements

Not applicable

References

1. Bray F, Ferlay J, Soerjomataram I, Siegel RL, Torre LA, Jemal A. Global cancer statistics 2018: GLOBOCAN estimates of incidence and mortality worldwide for 36 cancers in 185 countries. *CA: a cancer journal for clinicians* 2018, **68**(6)**:** 394-424.
2. Brenner H, Kloor M, Pox CP. Colorectal cancer. *Lancet (London, England)* 2014, **383**(9927)**:** 1490-1502.
3. Siegel RL, Miller KD, Fedewa SA, Ahnen DJ, Meester RGS, Barzi A*, et al.* Colorectal cancer statistics, 2017. *CA: a cancer journal for clinicians* 2017, **67**(3)**:** 177-193.
4. Lekka E, Hall J. Noncoding RNAs in disease. *FEBS letters* 2018, **592**(17)**:** 2884-2900.
5. Beermann J, Piccoli MT, Viereck J, Thum T. Non-coding RNAs in Development and Disease: Background, Mechanisms, and Therapeutic Approaches. *Physiological reviews* 2016, **96**(4)**:** 1297-1325.
6. Taft RJ, Pheasant M, Mattick JS. The relationship between non-protein-coding DNA and eukaryotic complexity. *BioEssays : news and reviews in molecular, cellular and developmental biology* 2007, **29**(3)**:** 288-299.
7. Sanger HL, Klotz G, Riesner D, Gross HJ, Kleinschmidt AK. Viroids are single-stranded covalently closed circular RNA molecules existing as highly base-paired rod-like structures. *Proceedings of the National Academy of Sciences of the United States of America* 1976, **73**(11)**:** 3852-3856.
8. Cocquerelle C, Mascrez B, Hétuin D, Bailleul B. Mis-splicing yields circular RNA molecules. *FASEB journal : official publication of the Federation of American Societies for Experimental Biology* 1993, **7**(1)**:** 155-160.
9. Meng S, Zhou H, Feng Z, Xu Z, Tang Y, Li P*, et al.* CircRNA: functions and properties of a novel potential biomarker for cancer. *Molecular cancer* 2017, **16**(1)**:** 94.
10. Wei CY, Zhu MX, Lu NH, Liu JQ, Yang YW, Zhang Y*, et al.* Circular RNA circ_0020710 drives tumor progression and immune evasion by regulating the miR-370-3p/CXCL12 axis in melanoma. *Molecular cancer* 2020, **19**(1)**:** 84.
11. Du WW, Yang W, Liu E, Yang Z, Dhaliwal P, Yang BB. Foxo3 circular RNA retards cell cycle progression via forming ternary complexes with p21 and CDK2. *Nucleic acids research* 2016, **44**(6)**:** 2846-2858.
12. Zhang Y, Zhang XO, Chen T, Xiang JF, Yin QF, Xing YH*, et al.* Circular intronic long noncoding RNAs. *Molecular cell* 2013, **51**(6)**:** 792-806.
13. Legnini I, Di Timoteo G, Rossi F, Morlando M, Briganti F, Sthandier O*, et al.* Circ-ZNF609 Is a Circular RNA that Can Be Translated and Functions in Myogenesis. *Molecular cell* 2017, **66**(1)**:** 22-37.e29.
14. Pamudurti NR, Bartok O, Jens M, Ashwal-Fluss R, Stottmeister C, Ruhe L*, et al.* Translation of CircRNAs. *Molecular cell* 2017, **66**(1)**:** 9-21.e27.
15. Yang Y, Fan X, Mao M, Song X, Wu P, Zhang Y*, et al.* Extensive translation of circular RNAs driven by N(6)-methyladenosine. *Cell Res* 2017, **27**(5)**:** 626-641.
16. Yang H, Zhang H, Yang Y, Wang X, Deng T, Liu R*, et al.* Hypoxia induced exosomal circRNA promotes metastasis of Colorectal Cancer via targeting GEF-H1/RhoA axis. *Theranostics* 2020, **10**(18)**:** 8211-

8226.

17. Wang X, Zhang H, Yang H, Bai M, Ning T, Deng T*, et al.* Exosome-delivered circRNA promotes glycolysis to induce chemoresistance through the miR-122-PKM2 axis in colorectal cancer. *Mol Oncol* 2020, **14**(3)**:** 539-555.
18. Shang A, Gu C, Wang W, Wang X, Sun J, Zeng B*, et al.* Exosomal circPACRGL promotes progression of colorectal cancer via the miR-142-3p/miR-506-3p- TGF-β1 axis. 2020, **19**(1)**:** 117.
19. Seol HS, Akiyama Y, Shimada S, Lee HJ, Kim TI, Chun SM*, et al.* Epigenetic silencing of microRNA-373 to epithelial-mesenchymal transition in non-small cell lung cancer through IRAK2 and LAMP1 axes. *Cancer letters* 2014, **353**(2)**:** 232-241.
20. Panda PK, Patra S, Naik PP, Praharaj PP, Mukhopadhyay S, Meher BR*, et al.* Deacetylation of LAMP1 drives lipophagy-dependent generation of free fatty acids by Abrus agglutinin to promote senescence in prostate cancer. 2020, **235**(3)**:** 2776-2791.
21. Bertoli G, Cava C, Diceglie C, Martelli C, Rizzo G, Piccotti F*, et al.* MicroRNA-567 dysregulation contributes to carcinogenesis of breast cancer, targeting tumor cell proliferation, and migration. *Breast cancer research and treatment* 2017, **161**(3)**:** 605-616.
22. Han M, Hu J, Lu P, Cao H, Yu C, Li X*, et al.* Exosome-transmitted miR-567 reverses trastuzumab resistance by inhibiting ATG5 in breast cancer. *Cell death & disease* 2020, **11**(1)**:** 43.
23. Vo JN, Cieslik M, Zhang Y, Shukla S, Xiao L, Zhang Y*, et al.* The Landscape of Circular RNA in Cancer. *Cell* 2019, **176**(4)**:** 869-881.e813.
24. Glažar P, Papavasileiou P, Rajewsky N. circBase: a database for circular RNAs. *RNA (New York, NY)* 2014, **20**(11)**:** 1666-1670.
25. Jiang R, Li H, Yang J, Shen X, Song C, Yang Z*, et al.* circRNA Profiling Reveals an Abundant circFUT10 that Promotes Adipocyte Proliferation and Inhibits Adipocyte Differentiation via Sponging let-7. *Molecular therapy Nucleic acids* 2020, **20:** 491-501.
26. Dai X, Chen C, Yang Q, Xue J, Chen X, Sun B*, et al.* Exosomal circRNA_100284 from arsenite-transformed cells, via microRNA-217 regulation of EZH2, is involved in the malignant transformation of human hepatic cells by accelerating the cell cycle and promoting cell proliferation. *Cell death & disease* 2018, **9**(5)**:** 454.
27. Huang S, Li X, Zheng H, Si X, Li B, Wei G*, et al.* Loss of Super-Enhancer-Regulated circRNA Nfix Induces Cardiac Regeneration After Myocardial Infarction in Adult Mice. *Circulation* 2019, **139**(25)**:** 2857-2876.
28. Huang W, Fang K, Chen TQ, Zeng ZC, Sun YM, Han C*, et al.* circRNA circAF4 functions as an oncogene to regulate MLL-AF4 fusion protein expression and inhibit MLL leukemia progression. *Journal of hematology & oncology* 2019, **12**(1)**:** 103.
29. Huang XY, Zhang PF, Wei CY, Peng R, Lu JC, Gao C*, et al.* Circular RNA circMET drives immunosuppression and anti-PD1 therapy resistance in hepatocellular carcinoma via the miR-30-5p/snail/DPP4 axis. 2020, **19**(1)**:** 92.

30. Huang C, Liang D, Tatomer DC, Wilusz JE. A length-dependent evolutionarily conserved pathway controls nuclear export of circular RNAs. 2018, **32**(9-10)**:** 639-644.
31. Kristensen LS, Andersen MS, Stagsted LVW, Ebbesen KK, Hansen TB. The biogenesis, biology and characterization of circular RNAs. 2019, **20**(11)**:** 675-691.
32. Verduci L, Strano S, Yarden Y, Blandino G. The circRNA-microRNA code: emerging implications for cancer diagnosis and treatment. *Mol Oncol* 2019, **13**(4)**:** 669-680.
33. Eulalio A, Huntzinger E, Izaurralde E. Getting to the root of miRNA-mediated gene silencing. *Cell* 2008, **132**(1)**:** 9-14.
34. Djuranovic S, Nahvi A, Green R. A parsimonious model for gene regulation by miRNAs. *Science (New York, NY)* 2011, **331**(6017)**:** 550-553.
35. Galagali H, Kim JK. miRISC Composition Determines Target Fates in Time and Space. *Developmental cell* 2018, **47**(2)**:** 142-143.
36. Yu R, Yao J, Ren Y. A novel circRNA, circNUP98, a potential biomarker, acted as an oncogene via the miR-567/ PRDX3 axis in renal cell carcinoma. 2020.
37. Ferrara N, Adamis AP. Ten years of anti-vascular endothelial growth factor therapy. *Nature reviews Drug discovery* 2016, **15**(6)**:** 385-403.
38. Saharinen P, Eklund L, Pulkki K, Bono P, Alitalo K. VEGF and angiopoietin signaling in tumor angiogenesis and metastasis. *Trends in molecular medicine* 2011, **17**(7)**:** 347-362.
39. Nagy JA, Dvorak AM, Dvorak HF. VEGF-A and the induction of pathological angiogenesis. *Annual review of pathology* 2007, **2:** 251-275.
40. Holmes DI, Zachary I. The vascular endothelial growth factor (VEGF) family: angiogenic factors in health and disease. *Genome biology* 2005, **6**(2)**:** 209.
41. Claesson-Welsh L, Welsh M. VEGFA and tumour angiogenesis. *Journal of internal medicine* 2013, **273**(2)**:** 114-127.
42. Kim M, Jang K, Miller P, Picon-Ruiz M, Yeasky TM, El-Ashry D*, et al.* VEGFA links self-renewal and metastasis by inducing Sox2 to repress miR-452, driving Slug. *Oncogene* 2017, **36**(36)**:** 5199-5211.
43. Goos JA, de Cuba EM, Coupé VM, Diosdado B, Delis-Van Diemen PM, Karga C*, et al.* Glucose Transporter 1 (SLC2A1) and Vascular Endothelial Growth Factor A (VEGFA) Predict Survival After Resection of Colorectal Cancer Liver Metastasis. *Annals of surgery* 2016, **263**(1)**:** 138-145.

Tables

Table 1: Correlation between Circ_0030998 expression and clinicopathologic features of CRC patients.

Characteristics	Case number	Circ_0030998 expression		*p*-Value
		High (n=45)	Low (n=45)	
Gender				0.515
Male	56	26	30	
Female	34	19	15	
Age				0.509
≤50	32	18	14	
>50	58	27	31	
Tumor Location				0.832
Colon	50	24	26	
Rectum	40	21	19	
CEA				0.673
≤10ng/ml	43	23	20	
>10ng/ml	47	22	25	
Tumor size				0.09
≤5cm	49	20	29	
>5cm	41	25	16	
Lymph node metastasis				0.032*
Yes	53	32	21	
No	37	13	24	
TNM stage				0.028*
I-II	33	11	22	
III–IV	57	34	23	

*$p<0.05$

Table 2. Univariate and multivariate analysis of prognostic factors for overall survival in CRC patients.

Characteristics	Univariate analysis		multivariate analysis	
	HR	***P*-value**	**HR(95%CI)**	***P*-value**
Gender	0.02	0.888		
Age	0.022	0.883		
Tumor Location	2.427	0.119		
CEA	0.339	0.561		
Tumor size	0.942	0.332		
Lymph node metastasis	9.810	0.002**	3.738(0.811-17.235)	0.091
TNM stage	15.320	<0.001***	68.543(7.047-666.695)	<0.001***
Circ_0030998 expression	6.588	0.01*	0.224(0.074-0.682)	0.008**

*p<0.05, **p<0.01, *** p<0.001

Figures

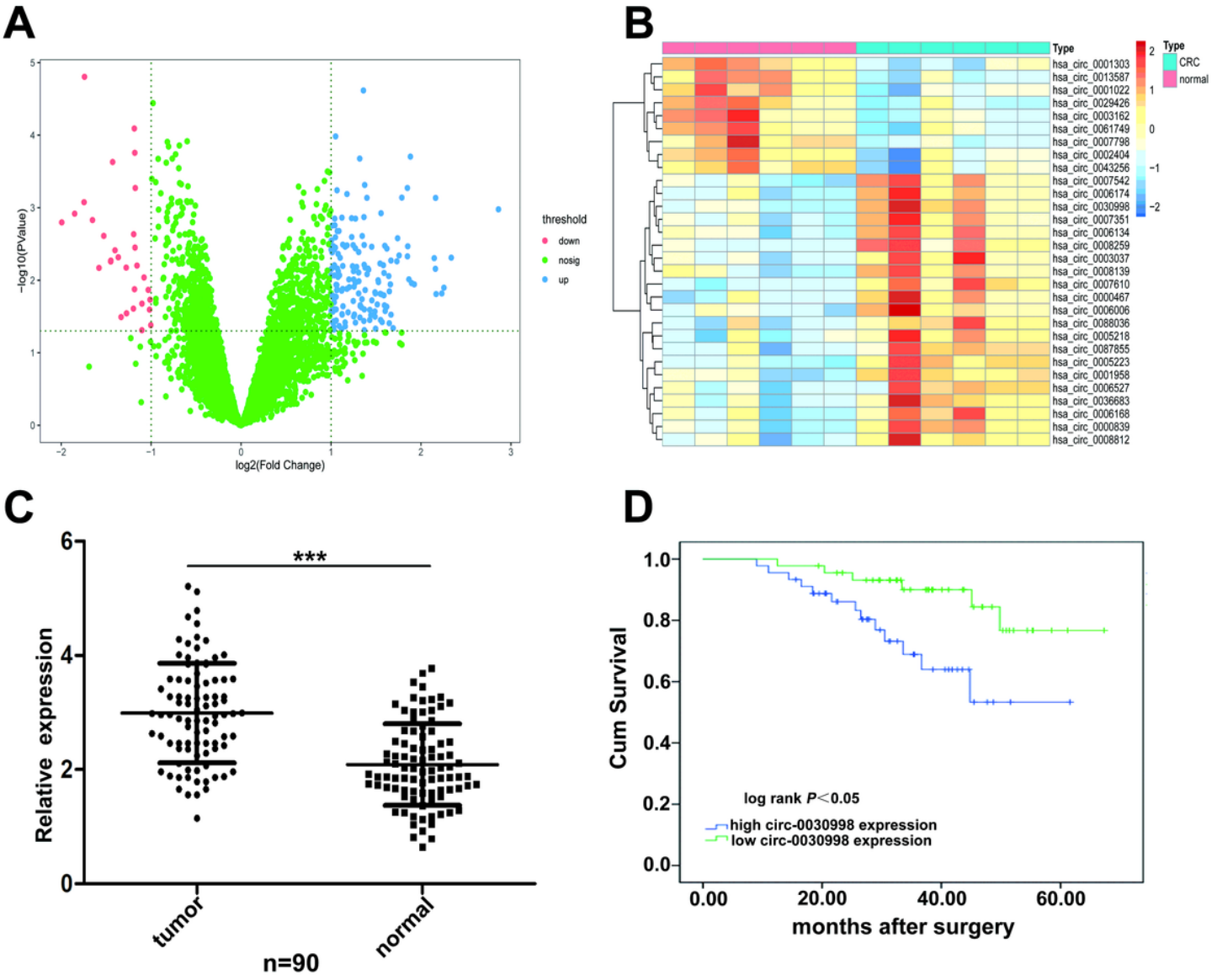

Figure 1

Circ_0030998 was upregulated in CRC tissues and associated with poor prognosis of CRC patients. A, The variation of CircRNAs expression between CRC tissues and matched neighboring normal tissues exhibited by the volcano plots generated from microarray data GSE138589. B, Heat map of the top 30 CircRNAs with the most significant differences from data GSE138589. C, Relative expression of Circ_0030998 in CRC tissues and paired adjacent normal tissues (n = 90). D, Correlation between Circ_0030998 expression and CRC patients' survival. ***p< 0.001.

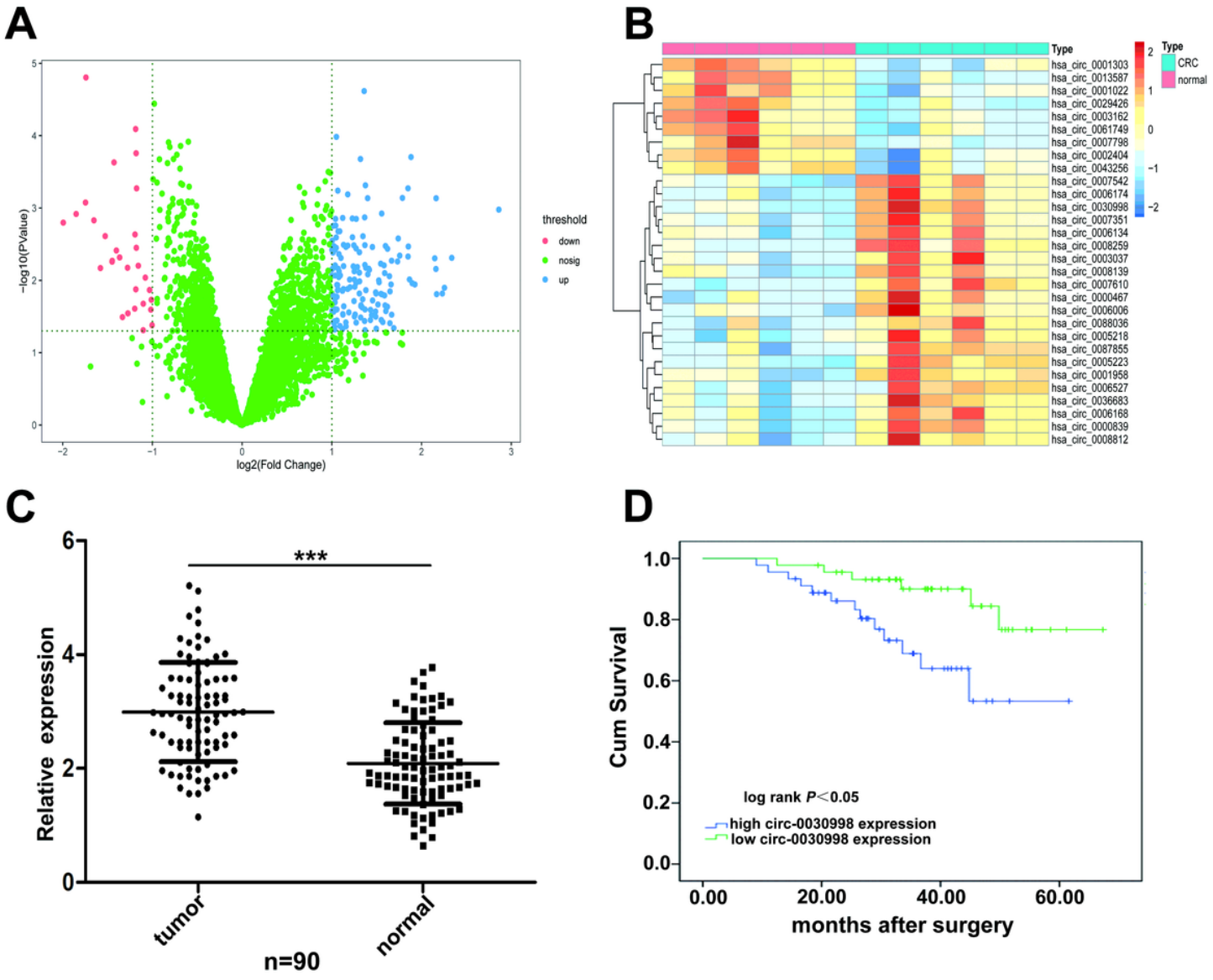

Figure 1

Circ_0030998 was upregulated in CRC tissues and associated with poor prognosis of CRC patients. A, The variation of CircRNAs expression between CRC tissues and matched neighboring normal tissues exhibited by the volcano plots generated from microarray data GSE138589. B, Heat map of the top 30 CircRNAs with the most significant differences from data GSE138589. C, Relative expression of Circ_0030998 in CRC tissues and paired adjacent normal tissues (n = 90). D, Correlation between Circ_0030998 expression and CRC patients' survival. ***p< 0.001.

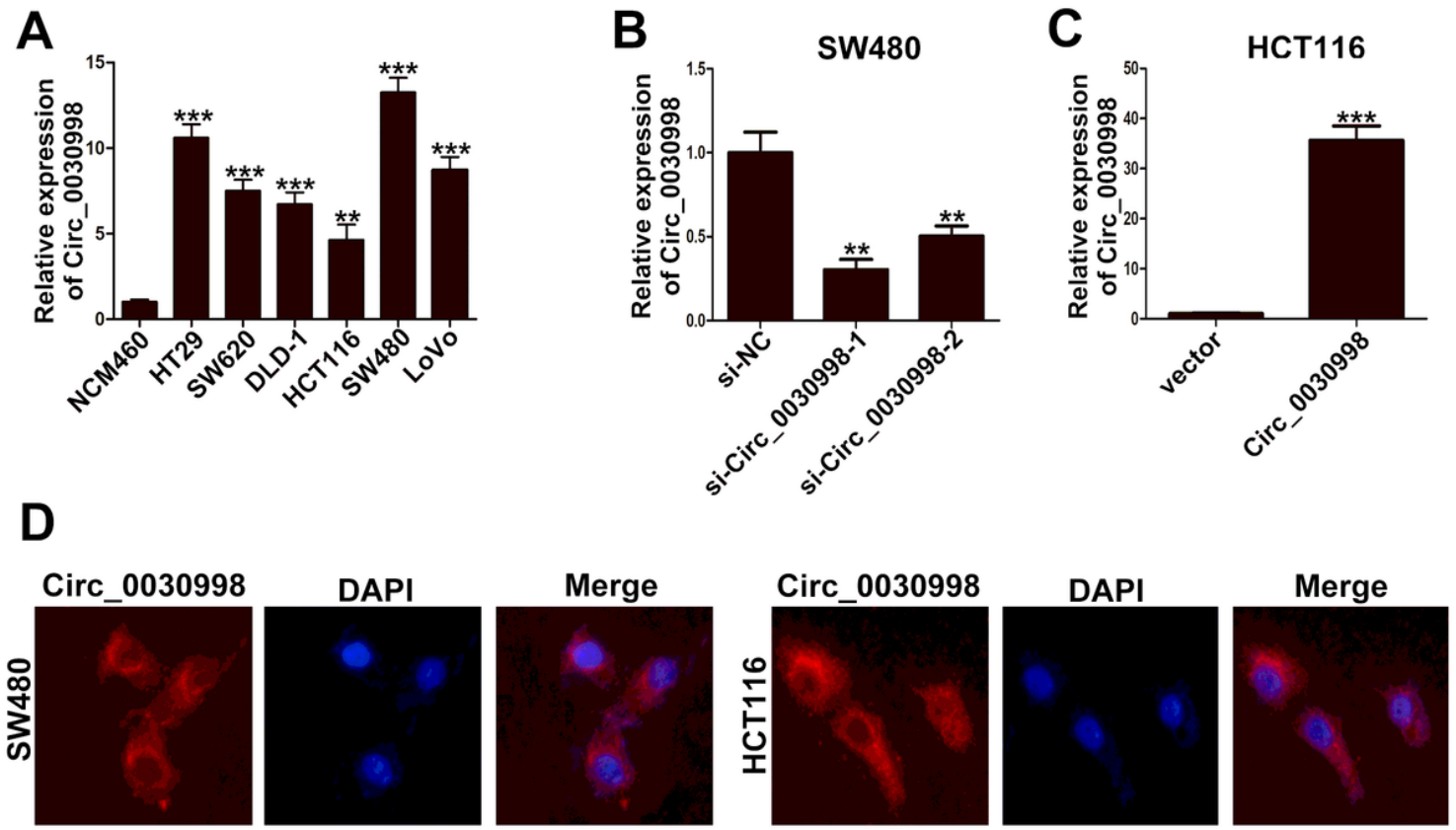

Figure 2

Circ_0030998 was upregulated in CRC cell lines and mainly localized in the cytoplasm of CRC cells. A, Relative expression of Circ_0030998 in CRC cell lines and human non-tumorigenic colorectal epithelial cell line NCM460 determined by qRT-PCR. B, The efficiency of siRNAs of Circ_0030998 in SW480 cells examined by qRT-PCR. C, The efficiency of pcDNA-Circ_0030998 in HCT116 cells examined by qRT-PCR. D, FISH images of Circ_0030998 expression in SW480 and HCT116 cells (red). Nuclei were stained by DAPI (blue). **p< 0.01, ***p< 0.001.

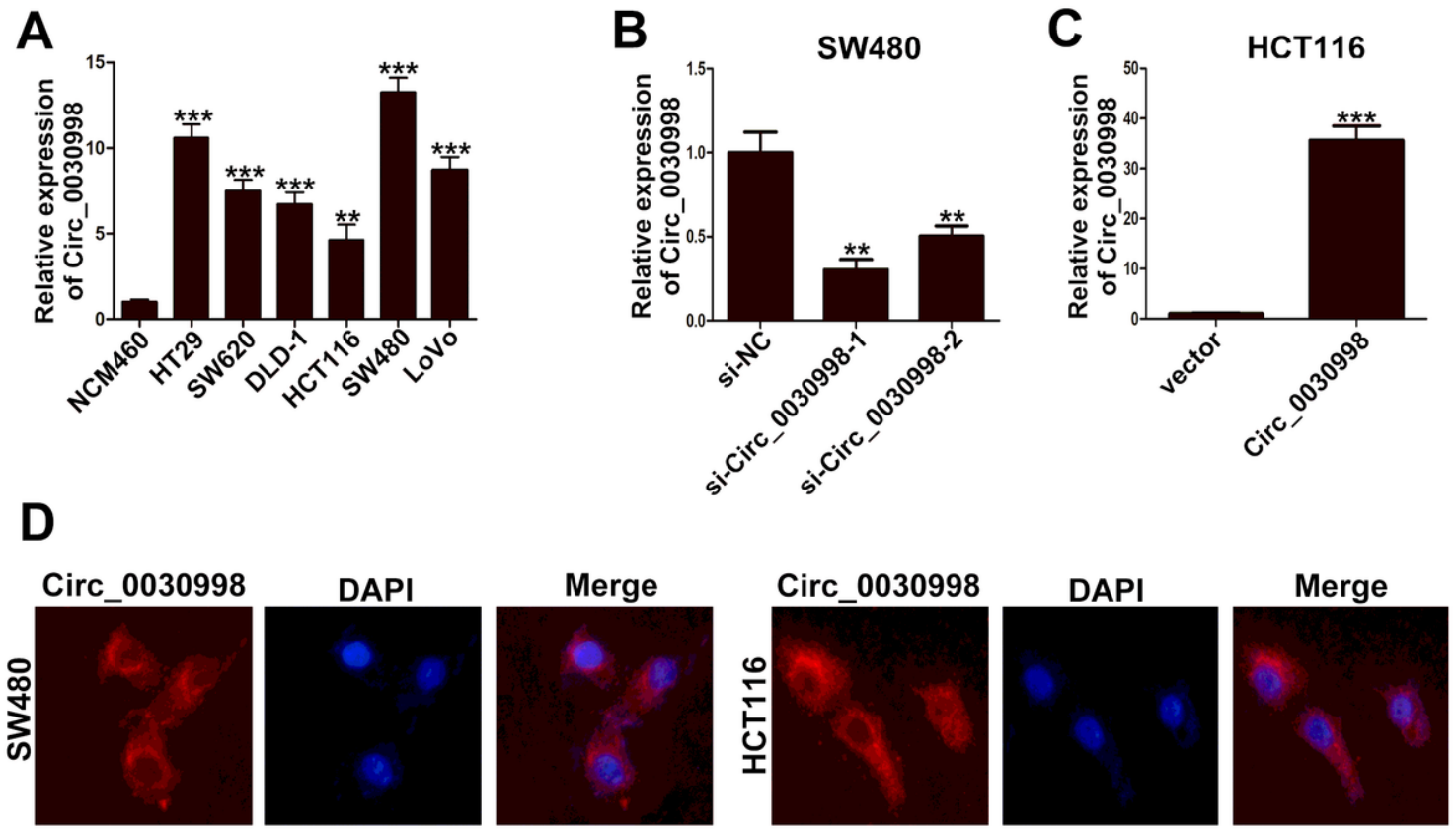

Figure 2

Circ_0030998 was upregulated in CRC cell lines and mainly localized in the cytoplasm of CRC cells. A, Relative expression of Circ_0030998 in CRC cell lines and human non-tumorigenic colorectal epithelial cell line NCM460 determined by qRT-PCR. B, The efficiency of siRNAs of Circ_0030998 in SW480 cells examined by qRT-PCR. C, The efficiency of pcDNA-Circ_0030998 in HCT116 cells examined by qRT-PCR. D, FISH images of Circ_0030998 expression in SW480 and HCT116 cells (red). Nuclei were stained by DAPI (blue). **p< 0.01, ***p< 0.001.

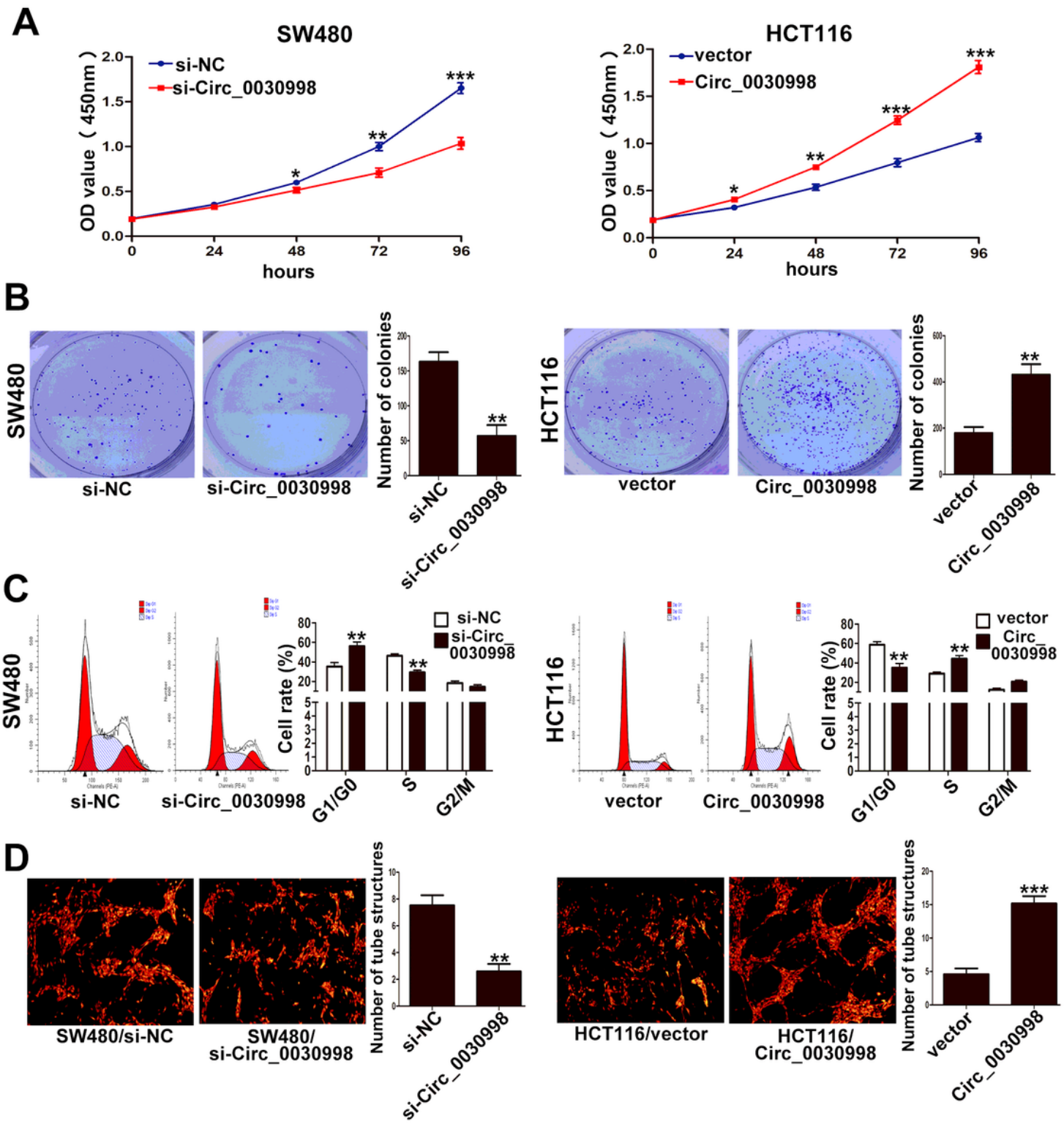

Figure 3

Circ_0030998 promoted CRC cells proliferation and angiogenesis in vitro. A, The proliferation ability of SW480 cells transfected with si-Circ_0030998 and HCT116 cells transfected with Circ_0030998 plasmid determined by CCK8 assays. B, The cloning ability of transfected SW480 and HCT116 cells. C, The effect of Circ_0030998 on cell cycle of SW480 and HCT116 cells. D, The tube-like structures of HUVECs cultured

in Matrigel-coated plates with conditioned medium from SW480 or HCT116 cells. *p< 0.05,**p< 0.01, ***p< 0.001.

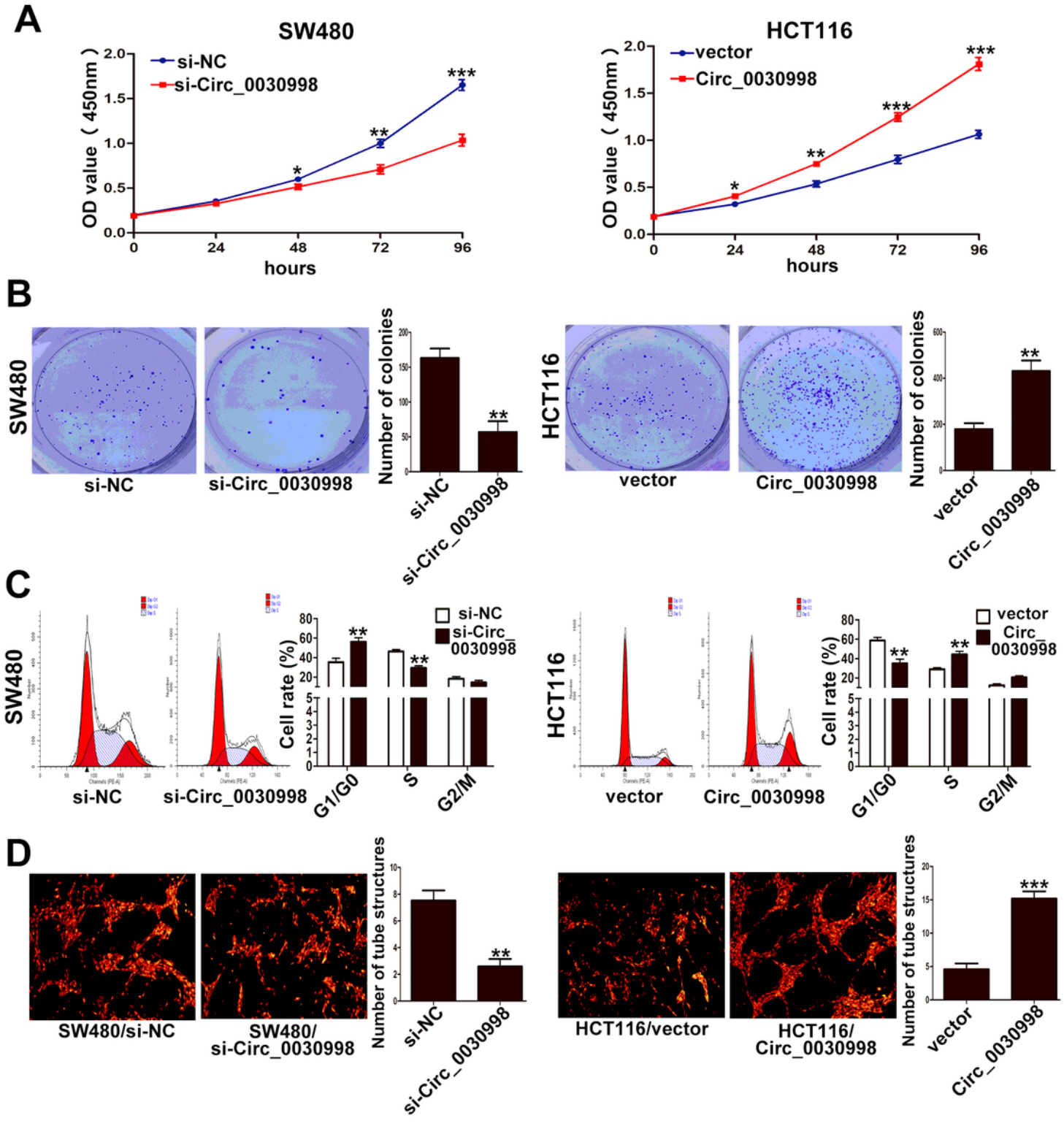

Figure 3

Circ_0030998 promoted CRC cells proliferation and angiogenesis in vitro. A, The proliferation ability of SW480 cells transfected with si-Circ_0030998 and HCT116 cells transfected with Circ_0030998 plasmid determined by CCK8 assays. B, The cloning ability of transfected SW480 and HCT116 cells. C, The effect

of Circ_0030998 on cell cycle of SW480 and HCT116 cells. D, The tube-like structures of HUVECs cultured in Matrigel-coated plates with conditioned medium from SW480 or HCT116 cells. *p< 0.05,**p< 0.01, ***p< 0.001.

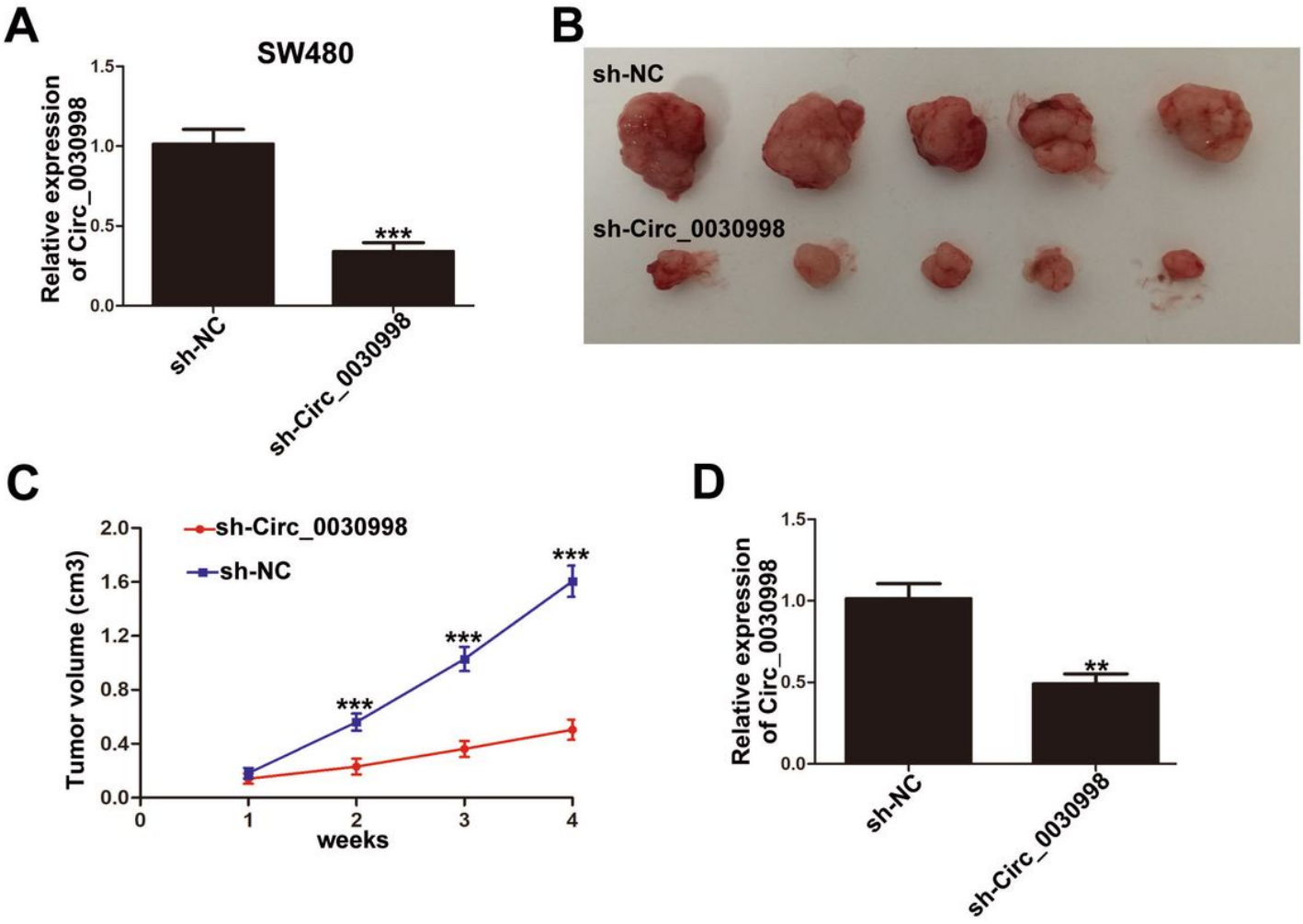

Figure 4

The effect of Circ_0030998 on CRC growth in vivo. A, The efficiency of sh-Circ_0030998 in SW480 cells examined by qRT-PCR. B, The tumor tissues from nude mice of SW480/sh-NC and SW480/sh-Circ_0030998 groups. C, The tumor volumes in two groups were evaluated every week until 4 weeks. D, The relative expression of Circ_0030998 in tumor tissues from two groups detected by qRT-PCR. **p< 0.01, ***p< 0.001.

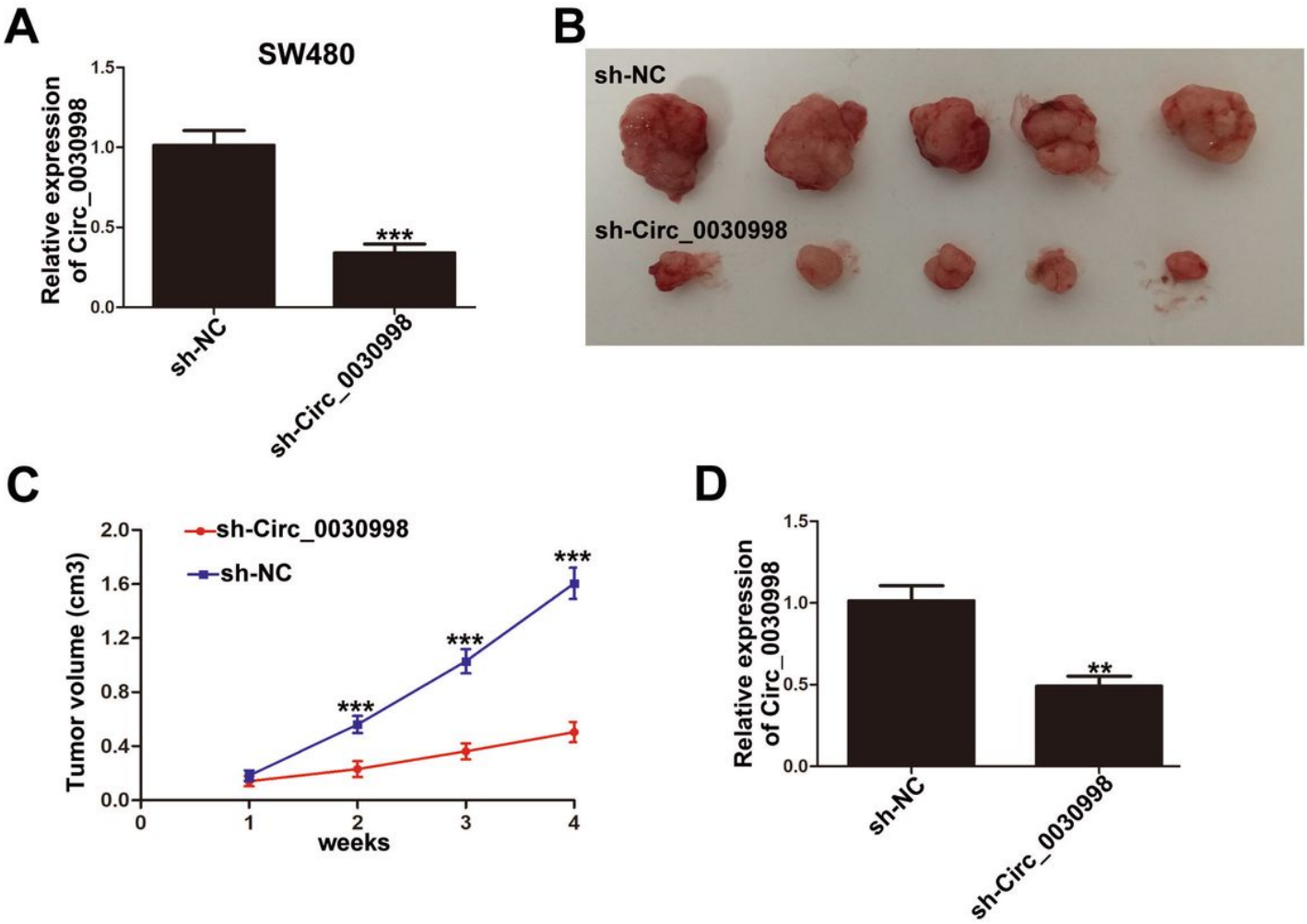

Figure 4

The effect of Circ_0030998 on CRC growth in vivo. A, The efficiency of sh-Circ_0030998 in SW480 cells examined by qRT-PCR. B, The tumor tissues from nude mice of SW480/sh-NC and SW480/sh-Circ_0030998 groups. C, The tumor volumes in two groups were evaluated every week until 4 weeks. D, The relative expression of Circ_0030998 in tumor tissues from two groups detected by qRT-PCR. **p< 0.01, ***p< 0.001.

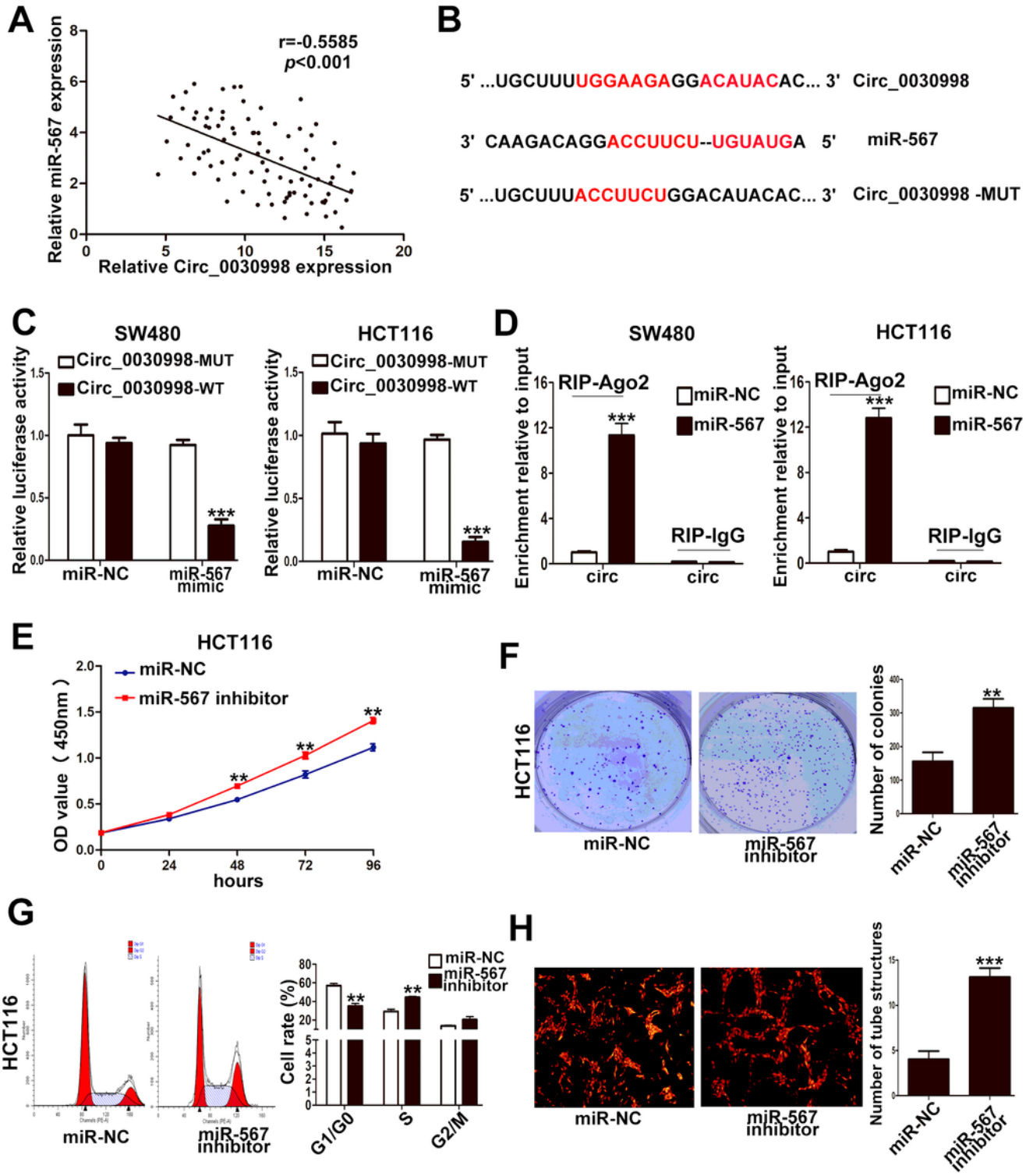

Figure 5

MiR-567 was a target of Circ_0030998 and inhibited the progression of CRC. A, The inverse correlation between miR-567 and Circ_0030998. B, The predicted binding sites of miR-567 and Circ_0030998. C, The results of the luciferase reporter assay validated the interaction between miR-567 and Circ_0030998. D, The level of Circ_0030998 enriched by RIP was detected in SW480 and HCT116 cells transfected with miR-567 or miR-NC. E, The effect of miR-567 on HCT116 cells proliferation determined by CCK8 assays. F,

The cloning ability of HCT116 cells transfected with miR-567 inhibitor. G, The effect of miR-567 on cell cycle of HCT116 cells. H, The tube-like structures of HUVECs cultured with conditioned medium from HCT116 cells. **p< 0.01, ***p< 0.001.

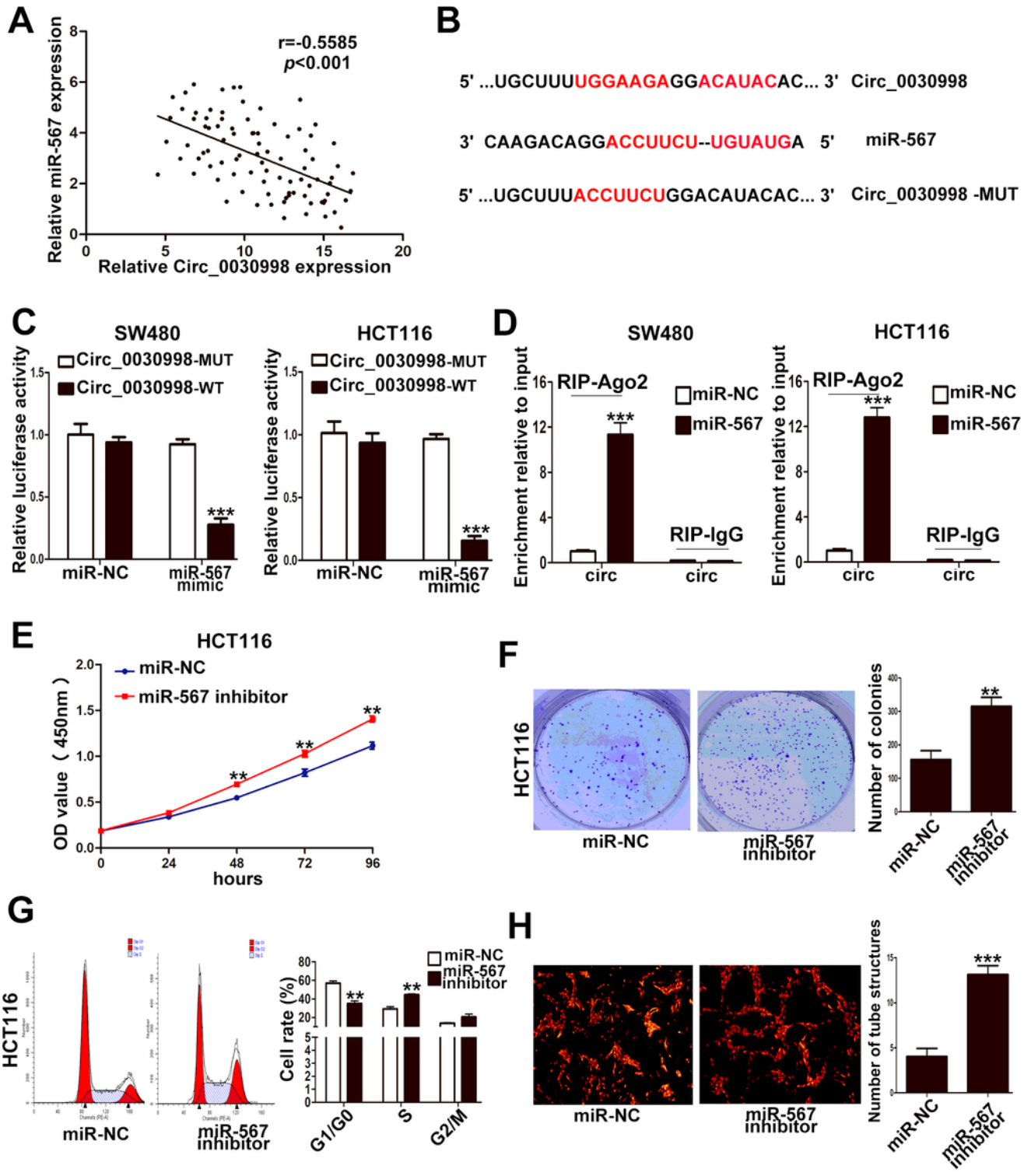

Figure 5

MiR-567 was a target of Circ_0030998 and inhibited the progression of CRC. A, The inverse correlation between miR-567 and Circ_0030998. B, The predicted binding sites of miR-567 and Circ_0030998. C, The

results of the luciferase reporter assay validated the interaction between miR-567 and Circ_0030998. D, The level of Circ_0030998 enriched by RIP was detected in SW480 and HCT116 cells transfected with miR-567 or miR-NC. E, The effect of miR-567 on HCT116 cells proliferation determined by CCK8 assays. F, The cloning ability of HCT116 cells transfected with miR-567 inhibitor. G, The effect of miR-567 on cell cycle of HCT116 cells. H, The tube-like structures of HUVECs cultured with conditioned medium from HCT116 cells. **p< 0.01, ***p< 0.001.

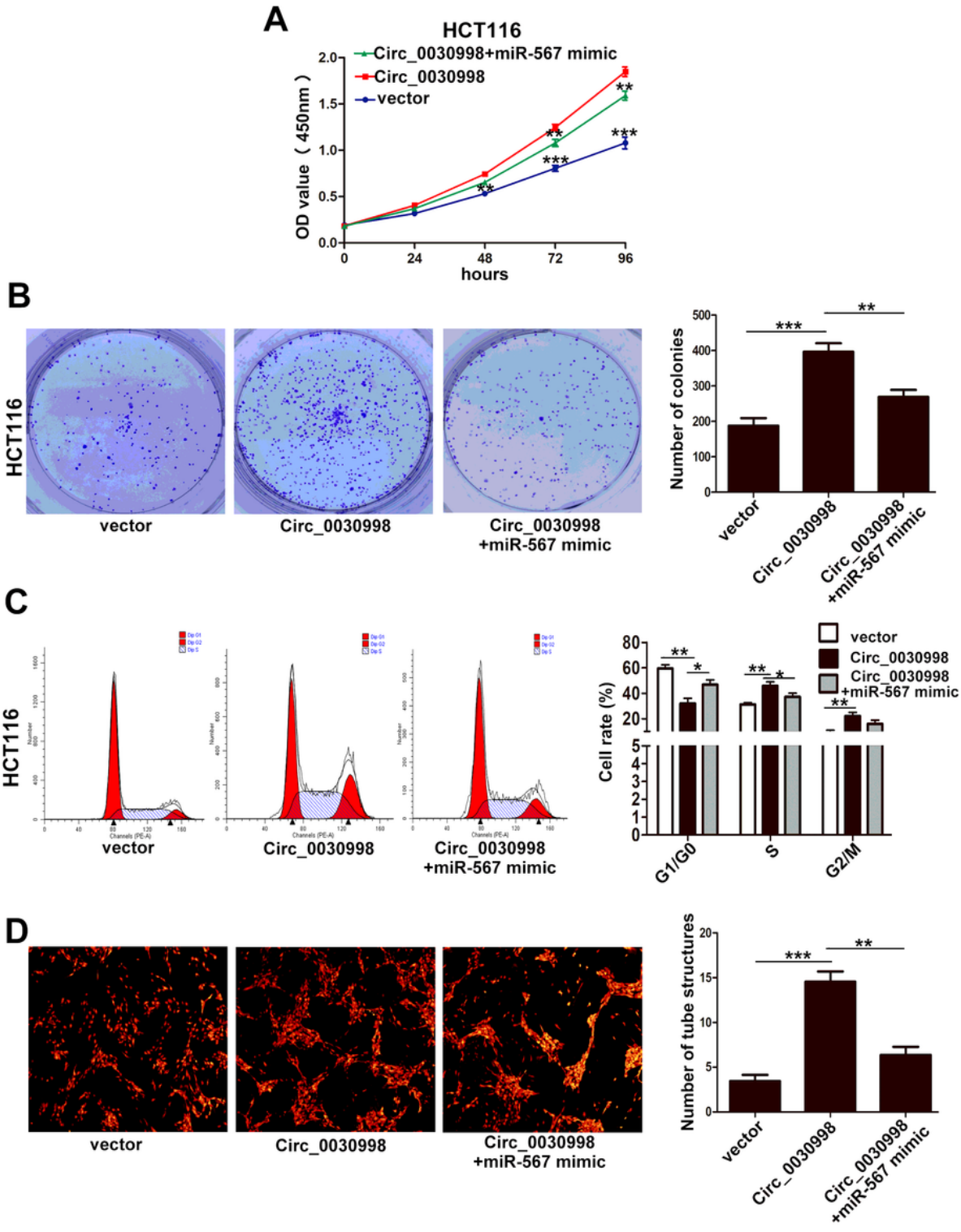

Figure 6

Circ_0030998 regulated CRC cells proliferation and angiogenesis via miR-567. A, The proliferation ability of HCT116 cells cotransfected with Circ_0030998 plasmid and miR-567 mimic. B, The cloning ability of cotransfected HCT116 cells. C, The cell cycle of cotransfected HCT116 cells. D, The tube-like structures of HUVECs cultured with conditioned medium from HCT116 cells. *p< 0.05,**p< 0.01, ***p< 0.001.

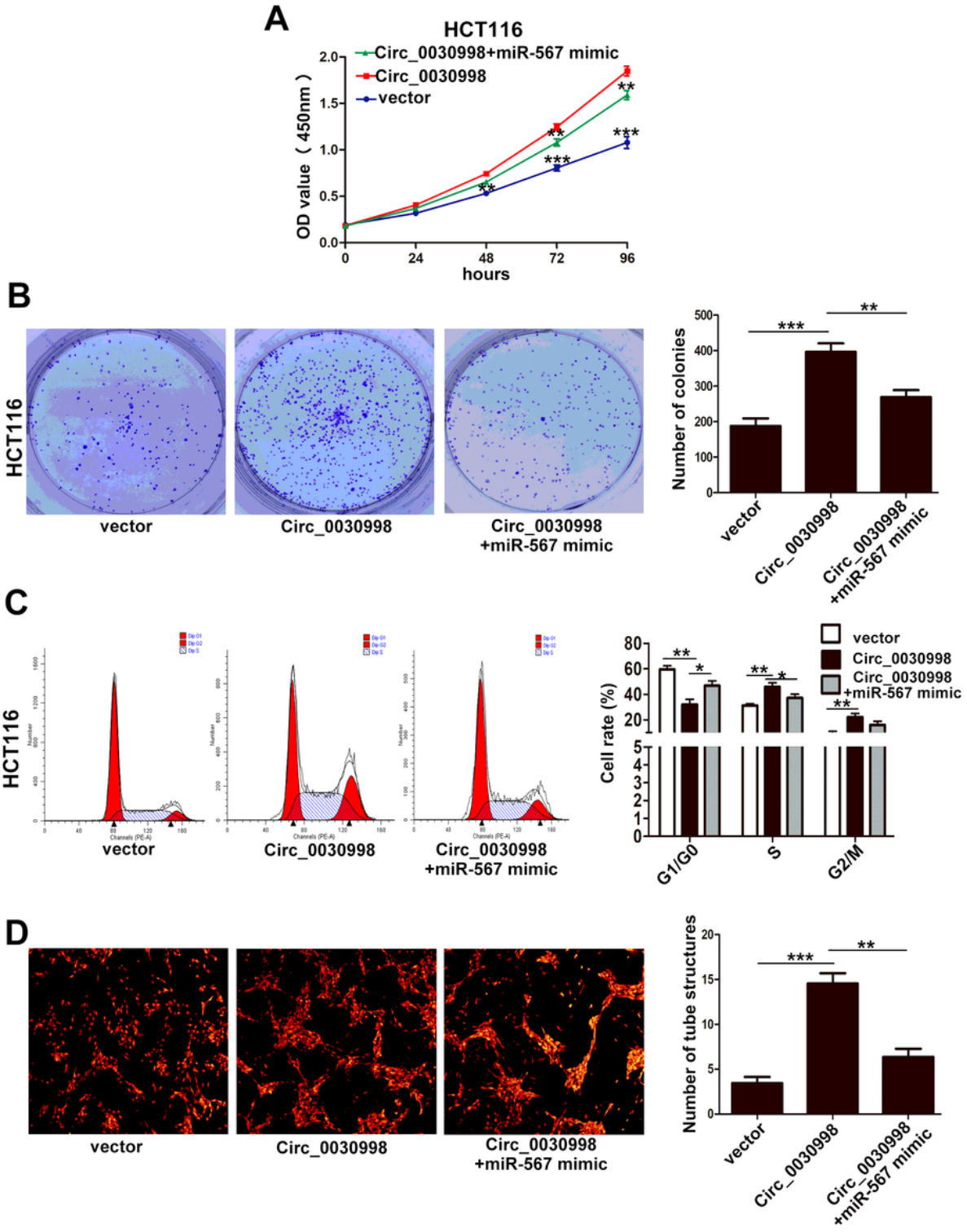

Figure 6

Circ_0030998 regulated CRC cells proliferation and angiogenesis via miR-567. A, The proliferation ability of HCT116 cells cotransfected with Circ_0030998 plasmid and miR-567 mimic. B, The cloning ability of cotransfected HCT116 cells. C, The cell cycle of cotransfected HCT116 cells. D, The tube-like structures of HUVECs cultured with conditioned medium from HCT116 cells. *p< 0.05,**p< 0.01, ***p< 0.001.

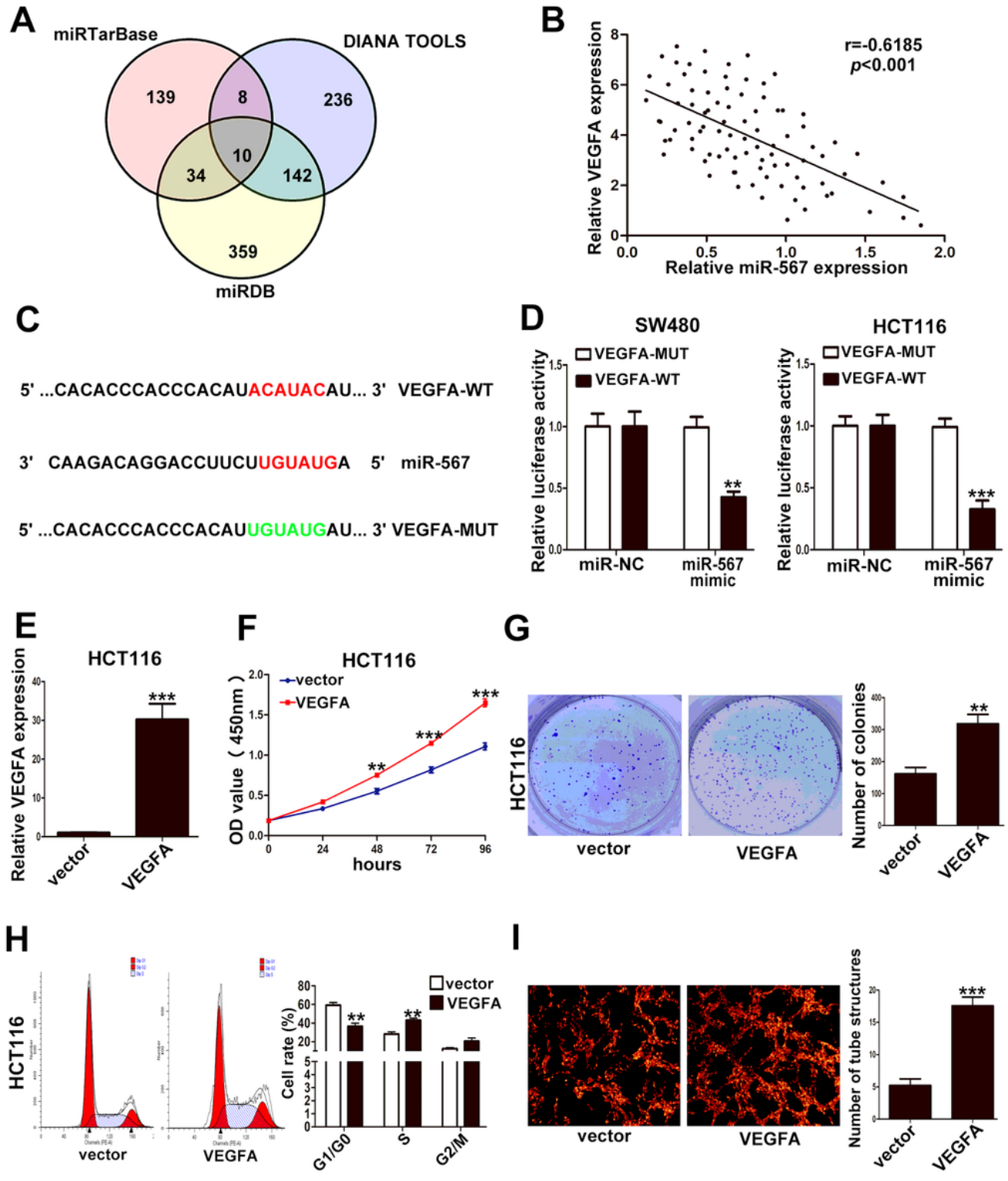

Figure 7

VEGFA was the target of miR-567 and promoted CRC cells proliferation and angiogenesis. A, The potential target genes of miR-567 predicted by three databases. B, The inverse correlation between miR-567 and VEGFA. C, The predicted binding sites of miR-567 and VEGFA. D, The results of the luciferase reporter assay validated the interaction between miR-567 and VEGFA. E, The efficiency of VEGFA plasmid in HCT116 cells examined by qRT-PCR. F, The effect of VEGFA on HCT116 cells proliferation determined by CCK8 assays. G, The effect of VEGFA on the cloning ability of HCT116 cells. H, The effect of VEGFA on cell cycle of HCT116 cells. I, The tube-like structures of HUVECs cultured with conditioned medium from HCT116 cells. **p< 0.01, ***p< 0.001.

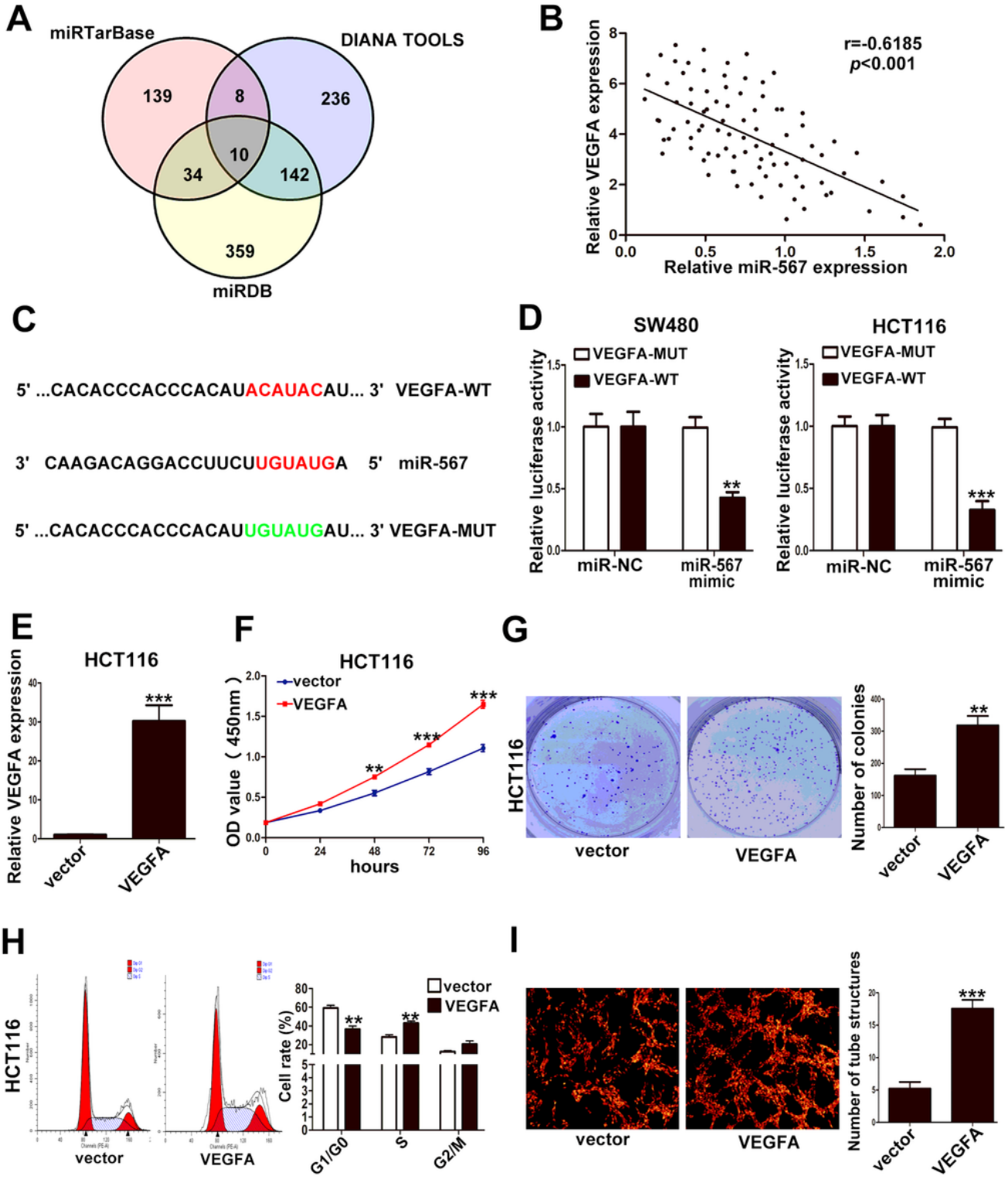

Figure 7

VEGFA was the target of miR-567 and promoted CRC cells proliferation and angiogenesis. A, The potential target genes of miR-567 predicted by three databases. B, The inverse correlation between miR-567 and VEGFA. C, The predicted binding sites of miR-567 and VEGFA. D, The results of the luciferase reporter assay validated the interaction between miR-567 and VEGFA. E, The efficiency of VEGFA plasmid in HCT116 cells examined by qRT-PCR. F, The effect of VEGFA on HCT116 cells proliferation determined

by CCK8 assays. G, The effect of VEGFA on the cloning ability of HCT116 cells. H, The effect of VEGFA on cell cycle of HCT116 cells. I, The tube-like structures of HUVECs cultured with conditioned medium from HCT116 cells. **p< 0.01, ***p< 0.001.

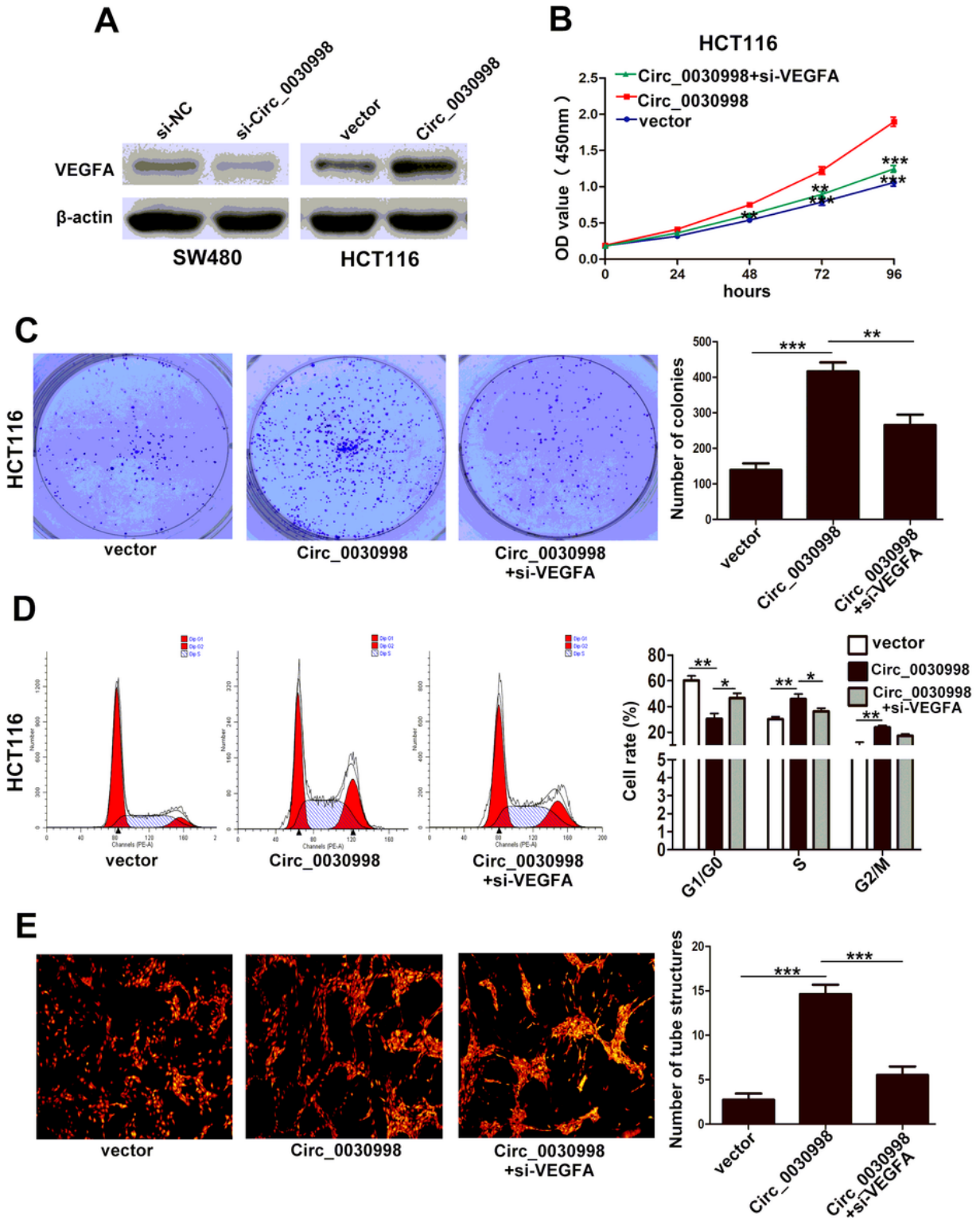

Figure 8

Circ_0030998 promoted CRC cells proliferation and angiogenesis relying on VEGFA. A, The effect of Circ_0030998 on the expression of VEGFA in CRC cells examined by western blotting. B, The proliferation

ability of HCT116 cells cotransfected with Circ_0030998 plasmid and si-VEGFA. C, The cloning ability of cotransfected HCT116 cells. D, The cell cycle of cotransfected HCT116 cells. E, The tube-like structures of HUVECs cultured with conditioned medium from HCT116 cells. *p< 0.05,**p< 0.01, ***p< 0.001.

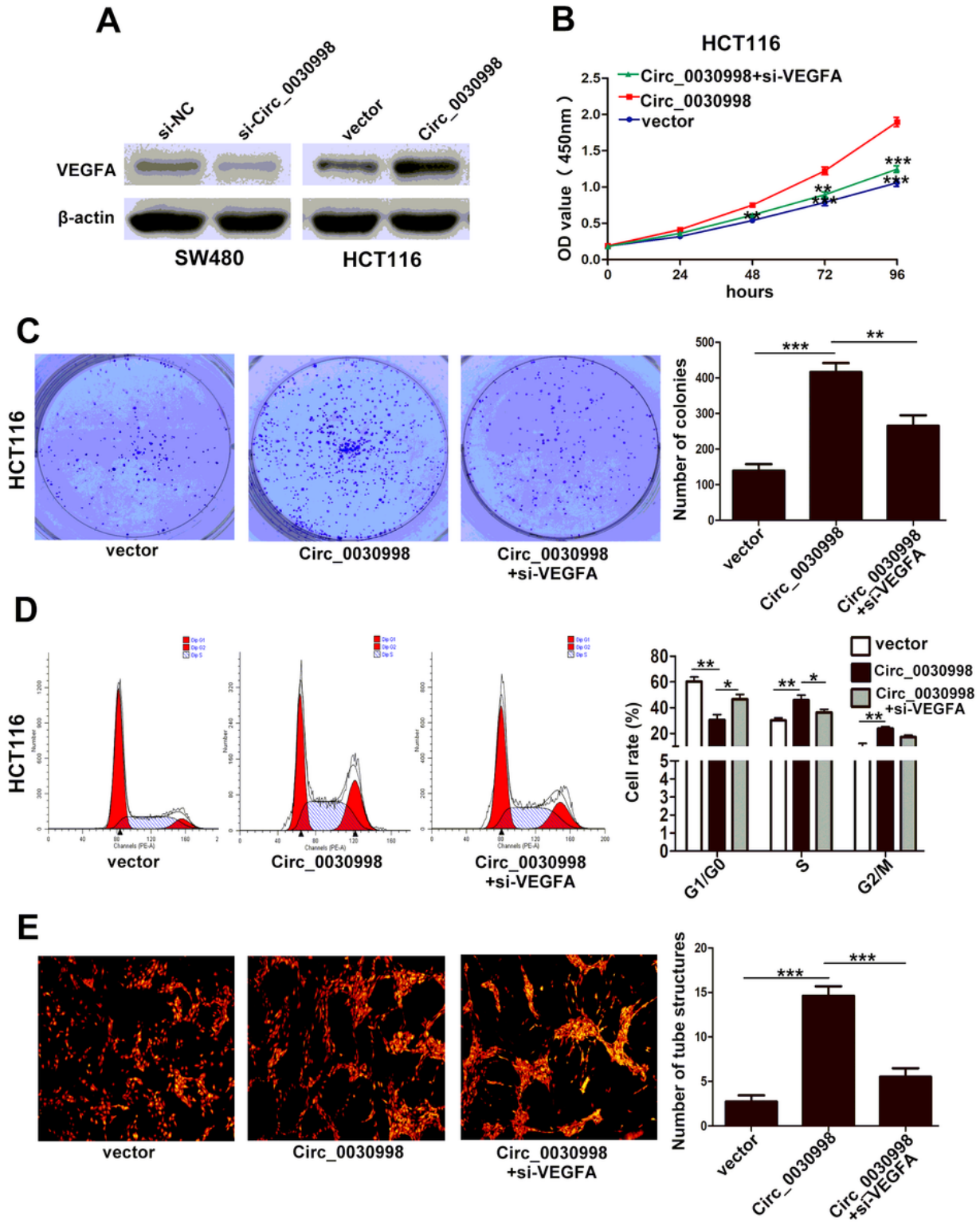

Figure 8

Circ_0030998 promoted CRC cells proliferation and angiogenesis relying on VEGFA. A, The effect of Circ_0030998 on the expression of VEGFA in CRC cells examined by western blotting. B, The proliferation

ability of HCT116 cells cotransfected with Circ_0030998 plasmid and si-VEGFA. C, The cloning ability of cotransfected HCT116 cells. D, The cell cycle of cotransfected HCT116 cells. E, The tube-like structures of HUVECs cultured with conditioned medium from HCT116 cells. *p< 0.05,**p< 0.01, ***p< 0.001.

Supplementary Files

This is a list of supplementary files associated with this preprint. Click to download.

- Highlights.docx
- Highlights.docx
- SupplementaryTable4.xlsx
- SupplementaryTable4.xlsx
- SupplementaryTable3.xlsx
- SupplementaryTable3.xlsx
- SupplementaryTable2.xlsx
- SupplementaryTable2.xlsx
- SupplementaryTable1.xlsx
- SupplementaryTable1.xlsx